The Development of Crestwing's Mechanical PTO System

Energiteknologisk udvikling og demonstration

1.1. Project Details

Project title	Development of Crestwing's mechanical PTO system
Project identification (program abbrev. and file)	12216
Name of the programme which has funded the project	energinet.dk with the ForskEl program.
Project managing company/institution (name and address)	Ruth Bloom Crestwing APS Silovej 8 9900 Frederikshavn
Project partners	
CVR (central business register)	34624100
Date for submission	July 31st 2019

1.2. Short Description of Project Objectives and Results

The purpose of this project is the development and documentation of a mechanical scalable PTO (Power Take-Off) system that can compete on efficiency and economy with PTO systems of the wind sector. The purpose is also to optimize the PTO system's ability to deliver smoothed electricity generation, unaffected by the frequency of incoming waves and wave trains.

This project has included results from Crestwing's half-scale vessel 'Tordenskiold', which has been tested at sea for five months during the Winter of 2018/19.

In general, the vessel, the anchorage, and the PTO system have managed the offshore tests in a very satisfactory manner. It can be deduced from the tests that:

- An idle bearing between the gear and generator must be installed.
- A brake function must be tested to determine the correct generator dimensioning.
- A new test should be conducted on the Tordenskiold PTO this Autumn with these changes.
- Further development of the flywheel is required.

Formålet med projektet er udvikling og dokumentation af et mekanisk skalerbart PTO-system som kan konkurrere på effektivitet og økonomi med vind sektorens PTO-systemer. Formålet er også optimering af PTO systemets evne til levering af en jævn elproduktion, som er upåvirket af frekvensen af de indkommende bølger og bølgetog.

Dette arbejde er udført på Crestwings halv skala anlæg Tordenskiold, som er blevet testet fem måneder vinteren over.

Generelt har anlægget, forankringen og PTO-systemet klaret offshore testene meget tilfredsstillende. Det kan bl.a. udledes af testene at:

- *Der skal monteres en friløbsleje imellem gear og generator.*
- *Der skal testes med en bremsefunktion for at afgøre generator størrelse.*
- *Der skal udføres en nye test i efteråret med disse ændringer.*
- *Yderlig udvikling af svinghjulene.*

Contents

1.3. Executive Summary

This project 12216 builds on Waveenergyfyn and Crestwing's other projects:

- 2008-2009 PSO-R&D Project no. 2008-1-110 110 and no. 10212 "Bølgevingen 1" and "Bølgevingen 2" test at AAU
- 2010-2011 PSO-R&D Project no.10465 “Crestwing final test” at DHI
- 2011-2014 PSO-R&D Project no. 10735 “Crestwing Final test follow-up offshore”
- 2012-2014 PSO-R&D Project no. 1080 “Detailed engineering and design of the WEC Crestwing”
- 2015-2018 PSO-R&D Project no. 12338 “Crestwing close to full scale”
- 2018-2020 Markedsmodningsfonden Project no. 2018-5819 “Bølgeenergikonceptet Crestwing offshore demonstration”

This project (12216) was originally approved by energinet.dk under the ForskEl program in 2013 with the purpose of the “development and documentation of a mechanically scalable PTO system that can compete on efficiency and economy with PTO systems of the wind sector. The purpose is also to optimize the PTO system's ability to deliver smooth electricity generation which is unaffected by the frequency of incoming waves and wave trains”.

The initial plan was to test and further develop the Power Take Off (PTO) system on which Waveenergyfyn in 2012 had manufactured and performed initial onshore tests. This testing was to be done using both on- and offshore tests. The onshore tests were to take place at AAU (Aalborg University), who would also analyse the resulting data.

In July 2014, Work package 1 Task 1.1 started, which was onshore testing at AAU, whereby the PTO system was set up on an AAU wave actuator and readied for testing. However, a misunderstanding occurred and AAU shut down the PTO system without completing any testing. Therefore Henning Pilgaard (the then director of Waveenergyfyn and subsequently Crestwing) chose to move to Task 1.6 and begin offshore tests.

A PTO system with power cabinet, inverter and dumpload, was installed in Wavenergyfyn's wooden model called ‘Fladstrand’, which had previously been tested at sea for three months without any problems in the Autumn of 2012. A new location for further testing was found, south of the naval station in Frederikshavn, where the model was laid out in September 2014. Unfortunately, on October 1st a storm struck and water entered the engine room, destroying the electrical components. Following this, Waveenergyfyn received an

extra grant from energinet.dk to repair the damage, and the PTO system was in for renovation by the manufacturer and a new electrical cabinet was ordered.

At the same time, Henning Pilgaard applied through his company Crestwing ApS, a grant from energinet.dk for the construction of a half-scale vessel which would run parallel to the onshore testing. The grant was given with a reduced budget, and the work began in January 2015.

The work on the half-scale vessel took all of Henning Pilgaard's time until his death on September 8, 2016. Following this, his wife and co-worker Ruth Bloom took over Crestwing ApS and continued the construction of the half-scale vessel.

In 2018, the ForskEl program was discontinued, the EUDP took over from energinet.dk, and made Crestwing aware that there was still a budget for the work to develop the PTO system. As the project still was absolute relevant, Crestwing resumed work on the PTO, but without the involvement of its previous partners, including DVE (who had supplied the generator, dumpload and inverter), Resen Energy, and AAU. Instead Crestwing employed the engineering consultancy firm, NIRAS, to analyse data from the offshore tests, and carry out onshore testing on the 2012 test bench to address the possibility of smoothing electricity generation from the PTO.

Unfortunately, the testbench failed in several areas including PLC, sensors, transmitters, and the generator which, due to saltwater penetration, showed faulty bearings, magnets, and windings. It was quickly estimated that the testbench would not be able to be used without new investments in components with associated long delivery times. Therefore, it was decided instead to make the appropriate measurements using the offshore model christened 'Tordenskiold'. This vessel is 30.0 m x 7.5m, weighs 65 tons, and consists of 2 pontoons, which are mechanically linked with hinges and a PTO shaft. In the engine room, power transmission equipment is installed which drives a generator that produces power. The system is equipped with monitoring equipment to monitor operating conditions, operational safety, wear, power production, and weather data. These measurements were used as input data for a mathematical model of the PTO, as a substitute for the onshore testing of the physical testbench. These changes were approved by the EUDP in the spring of 2019.

After the Tordenskiold off-shore test period, data collected were processed using the mathematical model, and the results are presented in this report. On the basis of these results, several possibilities have been investigated for smoothing electricity generation from the Tordenskiold, including active (using two flywheels

of different inertia and a control system), and passive (by linking the output of several vessels with an appropriate delay). In addition, the results indicate that the selected generator is too small to make any measurable impact on the passage of waves, and therefore the power output of the Tordenskiold could be significantly larger than is currently produced. Also, the results indicate that the flywheel is incapable of smoothing the power output of the PTO, and there are indications that there is some additional resistance in the PTO, creating a braking torque, which will be addressed during upcoming renovations.

There have been challenges in obtaining high-quality data to unambiguously show in which direction further development of the mechanical equipment can follow, and what the maximum amount of power can be extracted from the waves. However, the analysis of the data available indicates that changes and modifications to the design of the mechanical system should be made so as to achieve better interconnection between generator and flywheel, thereby enabling longer operation of the generator between waves, enabling the charging of on-board batteries. It has therefore been decided to carry out new measurements during the Autumn of 2019, after Tordenskiold has been in port and has undergone minor repairs with modifications as described in this report.

1.4. Project Objectives

The original project objective was to perform onshore tests on the mock-up of the Power-Take-Off (PTO) with a 3 kW generator that was built for Crestwing's 'Fladstand' model (that measured 10 m x 2,5 m and was built of wood). The PTO was exposed to sea-water during offshore testing and had been subsequently restored. However, when attempting to set up the PTO onshore for further testing, it transpired that the PTO was in poor condition. The most significant issues were as follows:

1. The data collection electronic hardware was incorrectly wired, and some components were entirely missing or broken. These were repaired where possible, and only strictly necessary components were used.

2. The PLC (Programmable Logic Controller) required to operate the PTO monitoring equipment was defective. This required a lengthy process of repair, involving the PLC manufacturer, software support, and a NIRAS electrician.

3. When actuating the hydraulic piston to drive the rack of the model PTO, it was found that the PTO produced a great deal of resistance – to the extent that it was feared that the PTO might violently

self-destruct. Testing was ceased until the source of the resistance was located. During this investigation, it was discovered that the generator linked to the PTO shaft was defective.

4. Attempts were made to either repair or replace the defective generator, but repair was impossible (determined by NordElectro, Frederikshavn), and no suitable replacement generator could be found within a reasonable time-frame.

It was concluded that additional components in the PTO might also be defective, and therefore the plan to use the onshore PTO mock-up was abandoned.

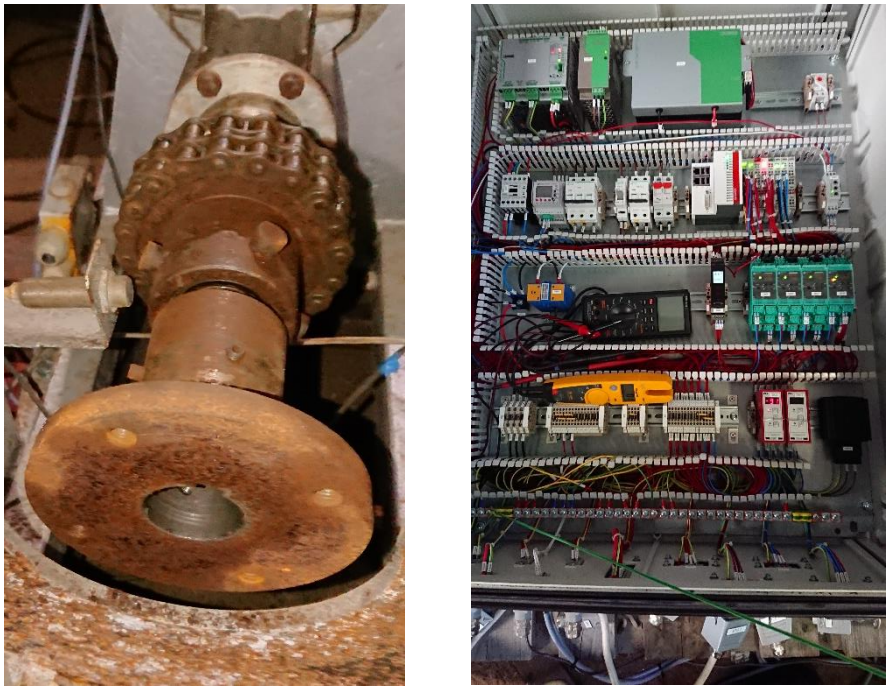

Figure 1. Left: Part of the test-bench PTO shaft, showing a high degree of corrosion. Right: Testing and re-wiring of the test-bench monitoring equipment.

In tandem with these efforts to test the on-shore PTO mock-up, was the launch of the half-scale Crestwing vessel, the 'Tordenskiold'. This was launched in waters of 20m depth off Frederikshavn, and was equipped with sensors to monitor the on-board PTO system. These data could be remotely monitored and downloaded for analysis. The PTO system in the Tordenskiold consists of a 20 kW generator with a span up to 30 kW, and a speed-up gear with a ratio of 1:5,09.

In February 2019, permission to modify the original project objectives and extend the project timespan was requested from the EUDP grant manager. These changes were accepted, and are as follows:

1. The data collected from the Tordenskiold is described, plus their analysis and limitations.

2. The technical possibilities for power smoothing are described, including the use of different mechanical and electrical power storage methods.

3. A mathematical simulation of the Tordenskiold PTO is developed as an alternative to the on-shore PTO mock-up.

4. Results from the mathematical simulation are analysed, and the model matched to the real data recorded from the Tordenskiold. In this way, an accurate simulation can be developed allowing for a reasonable assessment of the scalability of the PTO, in particular the generator output.

5. Suggestions of the most economically PTO set-up will be made.

1.5. Project Results and Dissemination of Results

1.5.1. Analysis of Real Data from Tordenskiold

1.5.1.1. Introduction

Throughout most of the course of this project period, the Tordenskiold has been at sea collecting data. It was brought to shore for maintenance and review in April 2019, since which time no additional data has been collected. However, historical data is available through an online portal, named 'Splunk', hosted by SPICA. This portal allows access to a variety of measurements, such as temperatures and rotational velocities of PTO components. However, this data is intended primarily for monitoring purposes, not for scientific analysis of data; the data sample rate is only 1 Hz, and there are frequent gaps in data.

An alternative method of retrieving data is available through a second portal, also hosted by SPICA, which allows the download of 5 Hz data from a sub-selection of the sensors. This higher frequency data recording is intended for the scientific analysis of the PTO's response to the sea state. These data are recorded over a 24 hr period, and then erased to be rewritten every night at midnight, meaning that any data must be retrieved within the 24 hr period of interest, and it cannot be recovered once erased.

Unfortunately, for the purposes for this study only the lower quality data was available. This was due to missing data for the sensors of greatest importance, and a misunderstanding of the availability of historic high-quality data. Due to the low sample rate of the available data points (1 Hz) and the relatively high frequency of the motion of the PTO (a peak-to-peak oscillation of about 5 seconds), the 1 Hz data is not of high enough quality for detailed analysis; the rapid changes in PTO response to passing waves cannot be

recorded at 1 Hz – simply too much information is missing, so that an accurate picture of the forces and movement of the PTO is impossible to infer.

However, the 1 Hz data can be broadly analysed to determine data trends, and the coarse 1 Hz signal can be mathematically modified for limited use in Simulink simulations.

1.5.1.2. Methods

Data was collected from the vessel over twenty minute periods when the weather was stable and the number of dump-loads applied to the generator output was varied from one to five. In doing this, the effect of load on the PTO system could be analysed in order to construct a more accurate simulation of the vessel, and to determine the effect of the generator supplying an electrical load on the performance of the vessel and PTO.

Figure 2. Photograph of the five 9 kW dumploads installed on the Tordenskiold.

Detailed analysis was made on March 22nd 2019, between 16:04 and 17:04, during which three 20 minute periods of data were recorded, each whilst 1, 3, and 5 dump-loads were engaged. A second period was analysed on March 23rd 2019, between 12:20 and 14:05. Two minutes of data from each end of the 20 minute data period were discarded to ensure the correct number of dump-loads were engaged.

The useful data returned were;

- Average PTO rod load (N)
- PTO rack displacement (mm)
- Generator power – a product of DC voltage and current (W)
- The number of dump-loads connected to the generator, which increased from 1 to the maximum of 5 in 20 minute periods
- The wind conditions for these 20 minute periods

NOTE: The generator shaft velocity (RPM) over the entire period could not be used as too much data was missing to be used as a complete data source.

Rack displacement is a measure of the distance travelled by the rack of the rack-and-pinion. It moves linearly back and forth along a rail as it is pushed and pulled by the rod. Its resting position should be at zero millimetres, therefore the data recorded from this element comprises both positive and negative values.

The rod load is a measure of the linear force developed along the PTO rod that is fixed between the two oscillating parts of the Tordenskiold vessel. One end is attached by a hinge directly to the body of one of these oscillating parts, whilst the other end is attached to the rack of the PTO. The relative motion of the two oscillating bodies is transformed to a horizontal linear motion by this rod, and into the PTO via the rack. The rod-load is therefore a direct measure of the amount of force being applied to the PTO, which is in turn a result of the height of the passing waves, and the resistance to motion of the PTO.

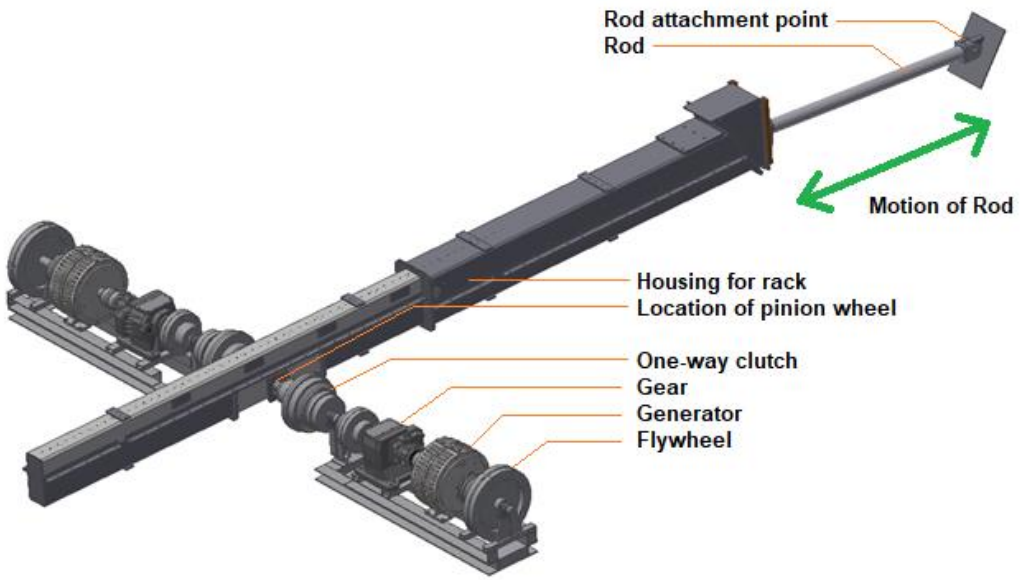

Figure 3. 3D rendering of the PTO designed for the Tordenskiold. Note that only one generator (and associated drive-train) is installed on the Tordenskiold.

The oscillating linear rack movement is then transformed to oscillating rotational movement by the pinion wheel. The pinion wheel drives the shaft of the drive-train, the first of which is a one-way clutch, which transmits rotation in only one direction. Thus, all subsequent elements of the drive train, including the generator and flywheel, are turned only in one direction. This one-way motion of the drive train is a fundamental aspect of the Crestwing's design, as it draws power from the wave only as the vessel 'falls' into the trough of a wave. As the vessel rises up to the peak of a wave, the PTO offers the absolute minimum of

resistance. Previous wave-pool tests on the Crestwing design have clearly indicated that a far greater power conversion is possible using this 'single-stroke' design (Crestwing 2008).

1.5.1.3. Results and Discussion

Rack displacement (mm), rod load (N), and generator power (W) are graphed below (figure 4, left to right), against the number of dumploads connected to the generator (1 to 3, and 1 to 5, in figures 4 and 5 respectively) for two dates. The rack displacement and rod load display the maximum positive values recorded, and also the range, i.e. the span between the maximum positive and the maximum negative values. The maximum and mean generator power (W) values are shown (there are no negative power values).

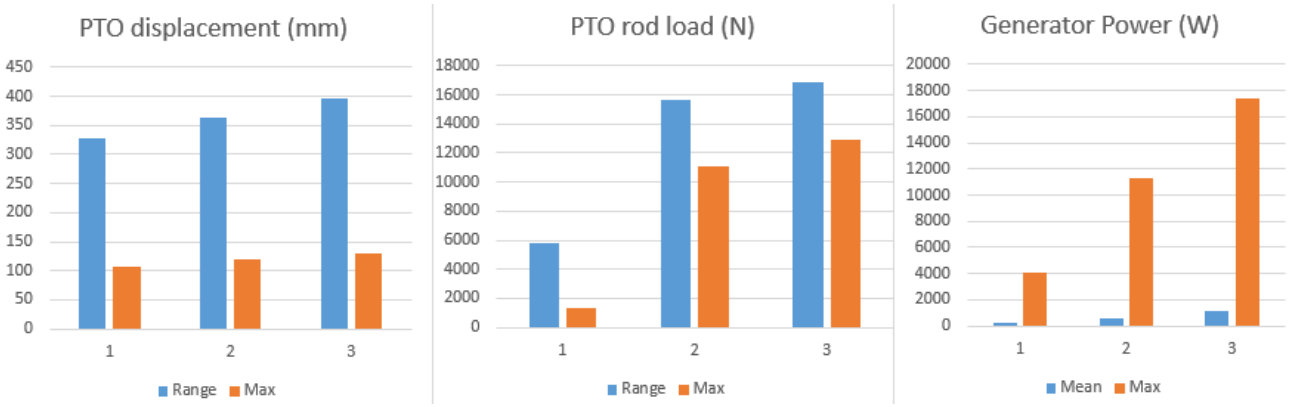

Figure 4. Maximum value and range/mean of three variables recorded over 16 (near) consecutive periods. Each chart displays the response to 1, 2, and 3 dumploads connected to the generator (left to right). Data recorded March 22nd 2019.

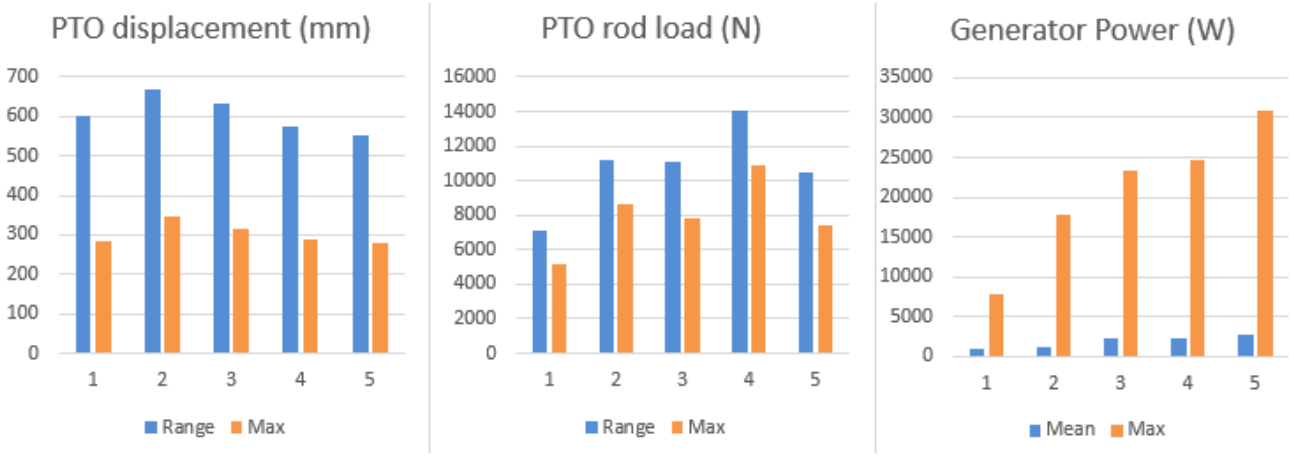

Figure 5. Maximum value and range/mean of three variables recorded over 16 (near) consecutive periods. Each chart displays the response to 1, 2, 3, 4, and 5 dumploads connected to the generator (left to right). Data recorded March 23rd 2019.

The above charts show a clear increase in generator power as the resistive load on the generator is increased, as is expected. However, the range and maximum PTO rack displacement shows no clear trend. A reduction in rack displacement might be expected if the increasing resistive load was impacting on the relative motion of the vessel's hinged barges. Figure 3 below graphically illustrates a 300 second sample of the raw data from which the above bar-charts were constructed. It represents the PTO rack displacement (mm) against time, with the black and red lines representing 1 and 5 loads respectively. No clear difference is apparent in the data.

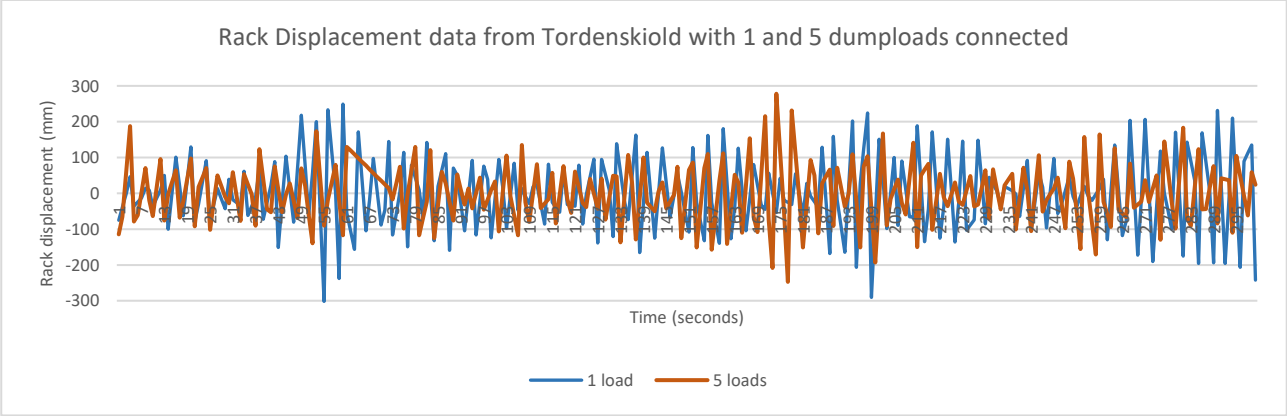

Figure 6. Representative 300 second period of the PTO rack displacement (mm) whilst the generator was connected to 1 (blue) and 5 dumploads. This serves to illustrate the similarities between the rack displacements regardless of the number of dumploads connected.

It is worth noting a larger-scale sinusoidal wave in figure 6 above, with a frequency of approximately 30 seconds. This suggests that the WEC vessel is resonating in and out of sync with the ocean wave frequencies, and losing power as a result when out of sync. This requires further investigation, and can be alleviated with a control mechanism such as latching, or varying the mechanical or electrical loads places on the generator to control its angular motion.

Another unexpected result from these data is that there is no clear increase in the PTO rod-force with increasing load. Using the second data set where the number of dumploads connected was increased from 1 to 5 in four steps, PTO rod force and PTO rack displacement show no corresponding change. This is illustrated in the figures below, where the coloured lines represent the data recorded for 1 (blue), 2 (dark green), 3 (light green), 4 (yellow), and 5 (red) connected dumploads, for a period of around 16 minutes. Each line is constructed from the addition of all absolute values within that time period (i.e. the positive values of each number recorded).

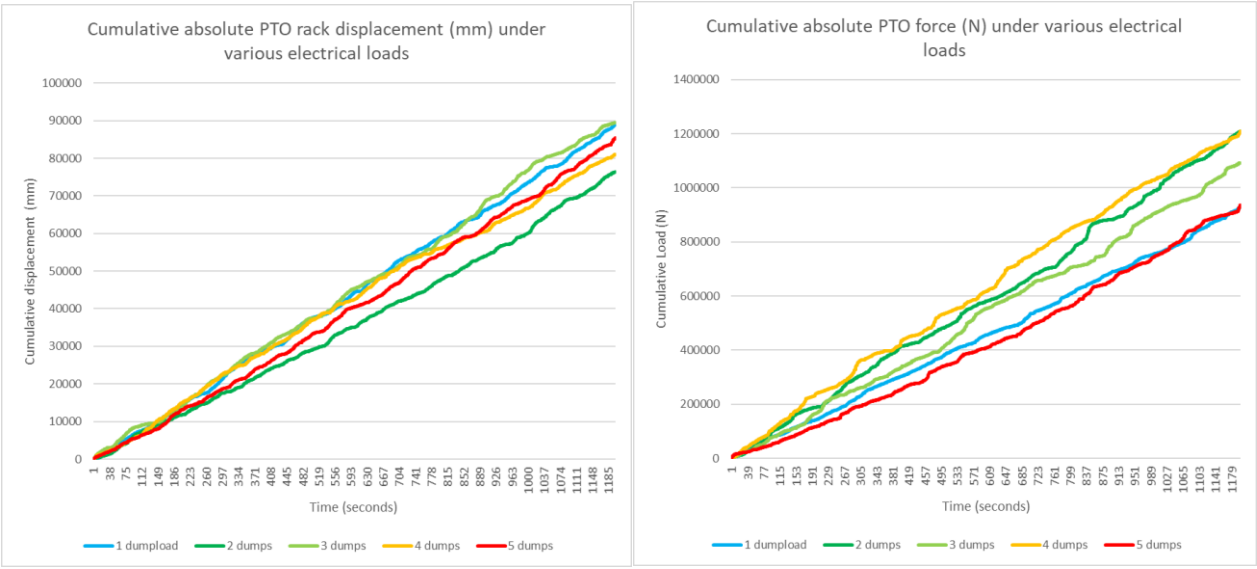

Figure 7. Cumulative absolute total values of PTO rack displacement (left) and force (right) with 1 to 5 dumploads connected to the generator.

The reason for analysing the data in this way is because there are doubts regarding the calibration and the zero point of the PTO load cell, i.e. there seems to be a systematic error in the data, whereby a zero load does not correspond to zero Newtons of force being recorded. Additionally, the force applied upon the rod to return the rack (i.e. when the one-way clutch has disengaged the PTO shaft) should be similar, regardless of the number of dumploads applied. Therefore, to include these values should influence each of the individual results equally. If the number of dumploads connected to the generator had an effect on either the rod force or the rack displacement, one would expect the slope of the lines (i.e. the cumulative total of force or displacement) to fall in a series – from 1 to 5. However, the results show no such pattern.

In addition to the directly recorded force and movement data, the rack's linear velocity (m/s) was calculated from the rack displacement (m) over time (s). This was then multiplied by the force recorded by the push rod's load sensor (N) to calculate the mechanical power input (W) to the PTO. These results were plotted against the electrical power output (W) from the generator for direct comparison (see figure 8 below).

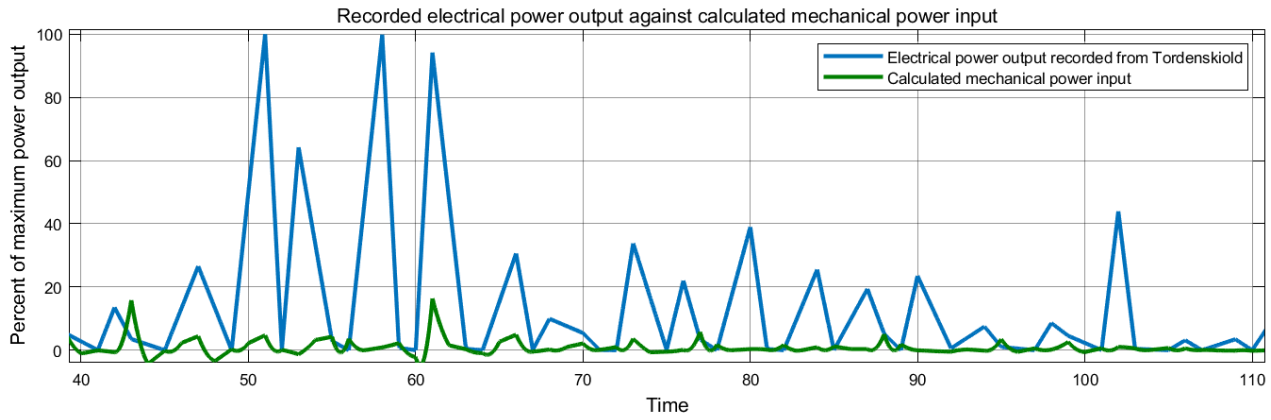

Figure 8. Seventy second sample of real data captured from the Tordenskiold. The blue line indicates the electrical output power of the generator, whilst the green line indicates the mechanical input power. The large discrepancies between the two are a result of the low data quality and/or incorrect sensor calibration.

From the above graph (of mechanical and electrical power) it is immediately clear that there is a poor data match, and the mechanical power input is lower than the electrical power output; a clear violation of the law of conservation of energy! This is most likely due to the data collection method favouring the capture of peak voltage and current (which are multiplied together to produce electrical power), whilst the calculated mechanical power relies upon averages values (over one second), which may greatly underestimate the peak mechanical power output.

In addition to the directly recorded data, the shaft torque (Nm) can be calculated from the product of the rod force (N) and the radius of the pinion wheel (0,071m). An example of this is graphed below.

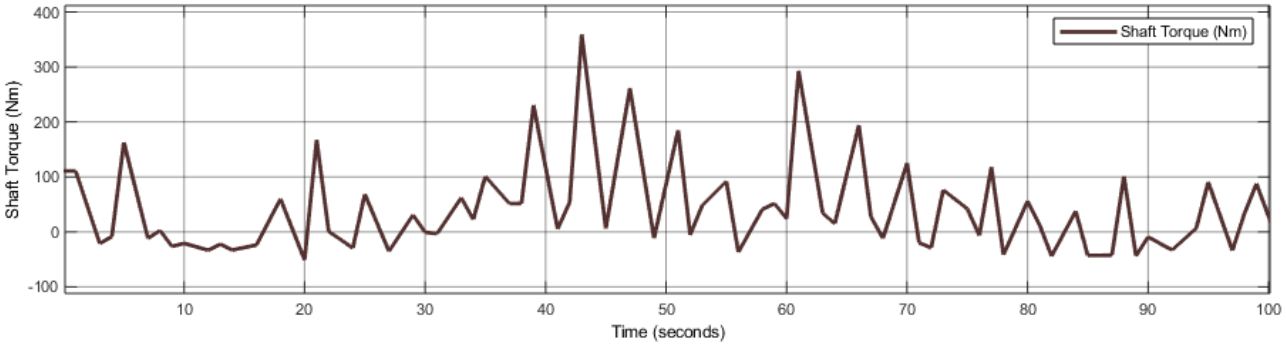

Figure 9. The shaft torque (Nm), before the one-way clutch. The data is from the same one-hundred second sample of real data from the Tordenskiold as in the figure directly above.

Using this method it is possible to calculate the maximum torque that the PTO shaft experienced whilst at sea, by finding the data from the highest seas. This was found to be January 1st 2019, where the rod load

reached a minimum of -9200 N, with a maximum of 530 N; a range of over 9700 N. However, when visualising these data, it is clear that there are inconsistencies (see graphs below).

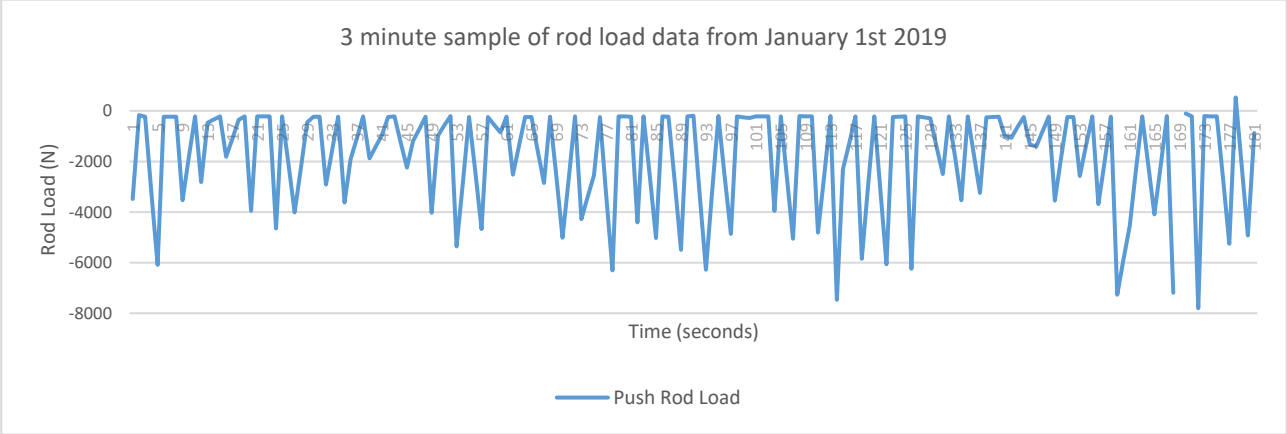

Figure 10. Three minute sample of data from the Tordenskiold on Jan 1st 2019. Note the near total absence of positive values of rod load.

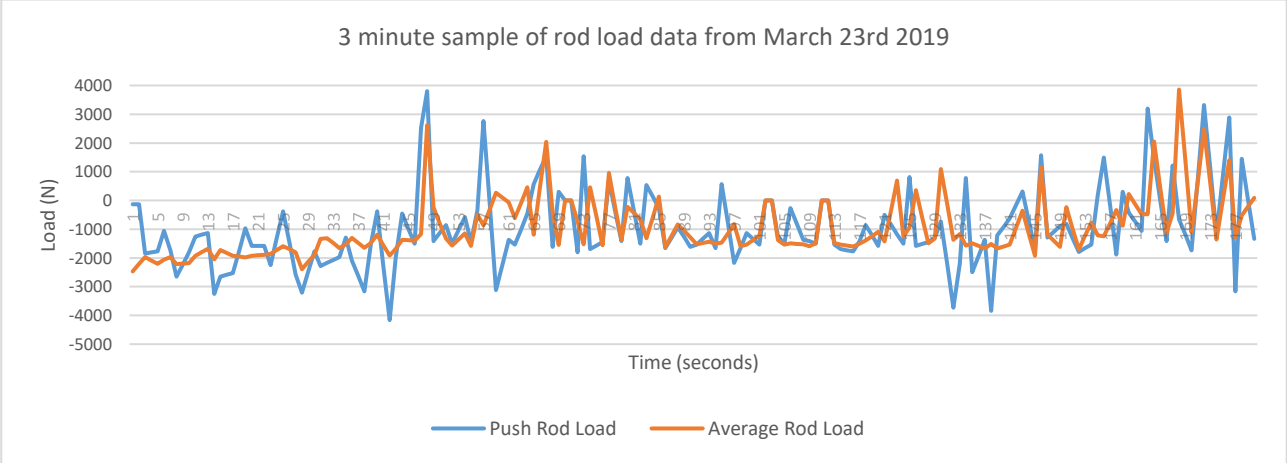

Figure 11. Three minute sample of data from the Tordenskiold on March 23rd. Note that the load values are both positive and negative and range around approximately -1500 N. Also illustrated is the 'average rod load' (orange) – another data set not available for the Jan 1st analysis. Note the broad similarities in terms of range and maximum values.

The push rod load (blue) is almost entirely of negative value in the Jan 1st data set, whilst this is not the case in the March 23rd data set. These inconsistencies call into question the validity of the data, making a reliable estimate of the maximum load, and thereby torque, impossible. In addition, the maximum rod load (non-corrected data) on March 23rd 2019 was in excess of 11.000 N.

If it is assumed that the vessel did experience a load of at least 9000 N, then that would equate to a torque on the PTO shaft of approximately 640 Nm. The torque on the generator shaft will be 5,09 times smaller than this, at approximately 125 Nm (due to the gearing; i=5,09. There will also be additional small losses not considered here).

1.5.1.4. Evaluation

This analysis demonstrates the following:

1. The 1 Hz data is not suitable for use to validate mathematical models of the Tordenskiold.
2. There may be an error in the data recording, or in terms of the calibration of the rod load-cells, leading to unexpected force values.
3. Calculations of torque values are not reliable, although peak torque levels of at least 640 Nm are not unreasonable, and are probably considerably greater.

1.5.2. Modelling of Changes in Flywheel Mass

1.5.2.1. Introduction

A flywheel is the current method of smoothing power on the Crestwing vessel, although it has proven to be ineffective in maintaining the necessary generator velocity between incoming waves to charge the on-board chemical batteries.

Flywheels are very simple in structure, and have very high efficiencies, high energy densities, with low costs. The rotational inertia of the mass of the flywheel allows kinetic energy to be stored which, in the case of an intermittent rotational velocity source such as that found in the Crestwing PTO, can be used to maintain and smooth the rotational velocity of a generator, thereby maintaining its speed closer to its nominal rated speed.

However, there is of course a trade-off associated with the use of flywheels; the greater the rotational inertia, the more force (torque) required to accelerate it. As such, a flywheel with large inertia will not be sped up quickly enough in small seas, whereas a flywheel with small inertia will not be capable of storing enough energy to effectively smooth out the power of irregular waves. This makes dimensioning a flywheel for very variable conditions extremely challenging.

1.5.2.2. Methods

Using Simulink, a model of the Tordenskiold 1:2 scale vessel was constructed. Simulink is a simulation software environment created by MathWorks which allows multi-domain integration of simulations, e.g. between physical and electronic systems, enabling the construction of realistic simulations of complete engineering systems. It has been used extensively in the renewable energy sector, particularly in wind energy, and many examples of Simulink models can be found online with a cursory search, that simulate systems as diverse as single islanded kilowatt turbines, to wind farms in the range of hundreds of megawatts.

Some assumptions had to be made regarding the resistance to motion of the dynamic elements of the vessel, but the dimensions, mass, and inertia were known for each component.

The rack displacement data recorded from the Tordenskiold was used as an input, after being transformed to linear velocity (m/s). Note that this transformation does not alter the underlying input data. This signal was translated to physical motion in the model, which was transmitted through the simulated PTO to a dynamic viscous damper, simulating the resistive torque of a generator under load.

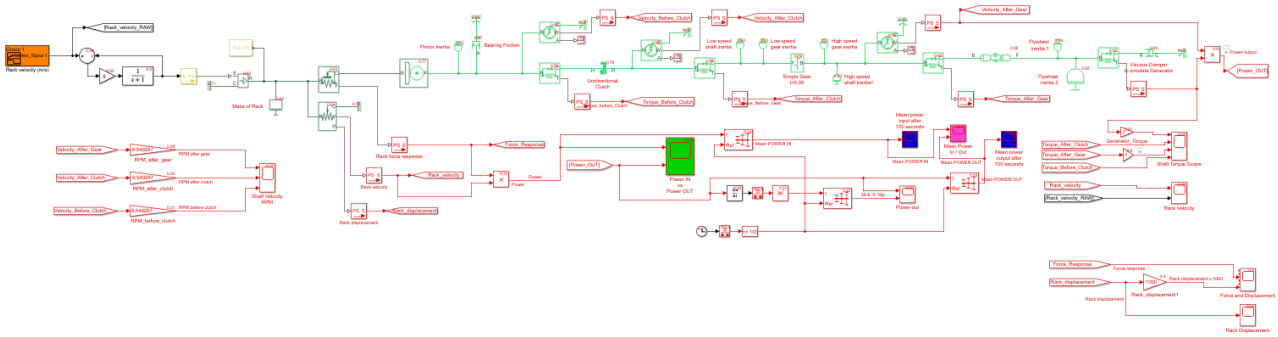

Figure 12. Simulink block diagram of the Tordenskiold PTO starting with the input force (left) and ending with power output scopes (right). For detailed model description, see the annex.

Figure 13. The flywheel currently installed on the Tordenskiold's PTO.

The rotational inertia of the flywheel currently installed on the Tordenskiold was calculated to be 8,4 kg*m^2, so the simulation was performed with this value as a base point. The rotational inertia was then raised to examine the effects upon the transmitted torque, the rotational velocity of the shaft elements, and ultimately the mechanical output power. The viscous damping effect was initially set at 10 N*m/(rad/s) as at this value the rotational velocity output of the simulation approximated that measured at the generator on the Tordenskiold. This value was also changed to represent changing electrical load, as too was the input signal gain, to simulate a change in the ocean wave amplitude.

1.5.2.3. Results

The simulated PTO shaft velocities are graphed below for the same 60 second period, applying low, mid, and high flywheel inertias; 8,4 kg*m^2, 16,8 kg*m^2, and 25,2 kg*m^2 respectively. They illustrate the input velocity (green; which has both positive and negative values as the pinion wheel rotates back and forth), the low-speed axel velocity (blue; after the one-way clutch but before the gear), and the high-speed axel velocity, which is the generator velocity.

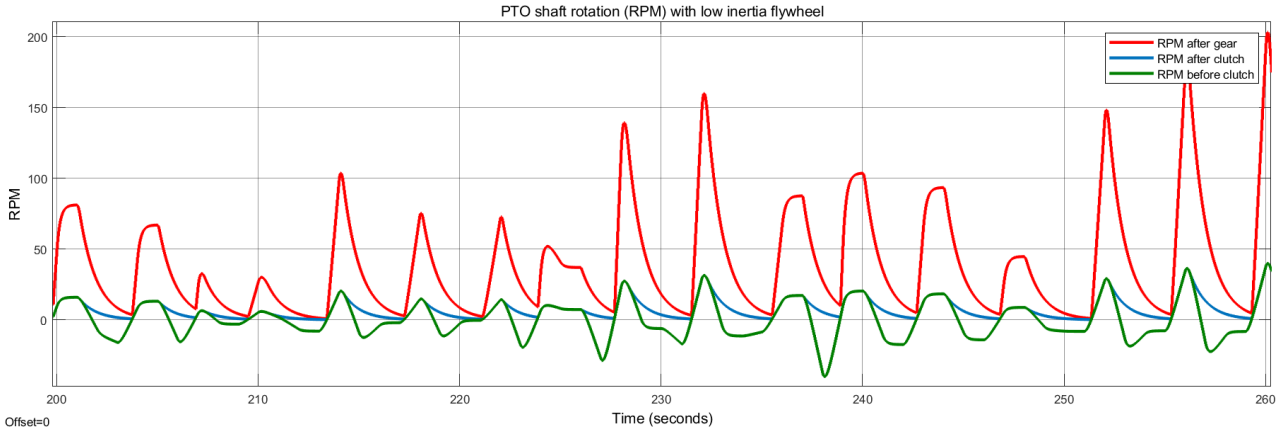

Figure 14. Low inertia (8,4 kg) flywheel simulation output, graphing the rotational velocity (RPM) of the PTO at the pinion wheel (green), after the one-way clutch (blue), and at the generator.

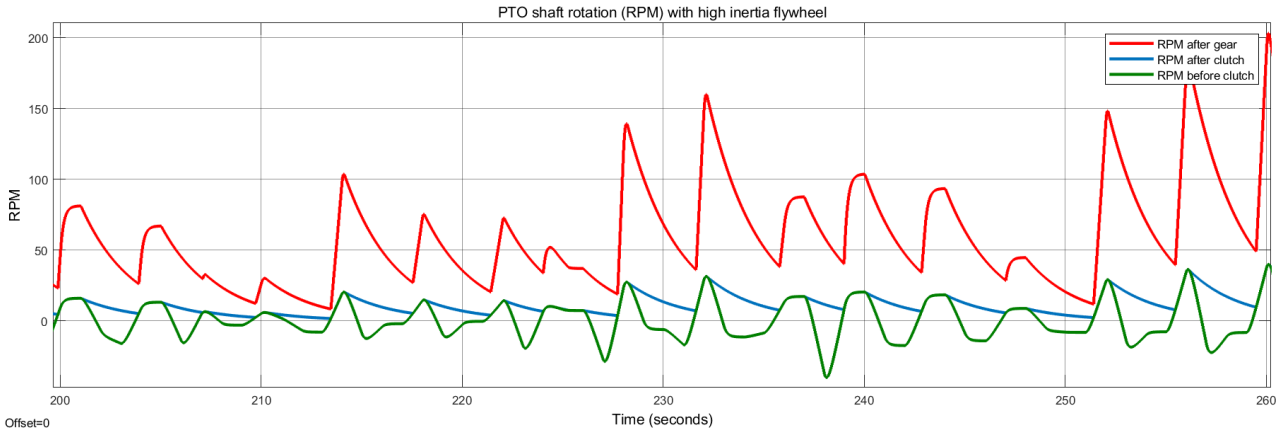

Figure 15. High inertia (25,2 kg) flywheel simulation output, graphing the rotational velocity (RPM) of the PTO at the pinion wheel (green), after the one-way clutch (blue), and at the generator.

The simulation uses an 'ideal velocity source', meaning that the input velocity (i.e. that of the pinion wheel) will not change with an increase in flywheel inertia; it is fixed, regardless of the resistance to motion. Whilst not ideal, this does replicate what is observed in the analysis of data from the Tordenskiold, i.e. an increased load on the generator has no measurable impact on its movement (at the load levels applied).

The response of the generator velocity to an increase in the flywheel inertia is seen in the continued rotation of the generator between successive 'pushes' from the waves. This is illustrated by the red line in the above figures, which does not return to zero in figure 15 (it does in figure 14), as the rate of velocity loss is reduced – a result of the higher inertia of the larger flywheel.

At a low damping coefficient (10 N*m/(rad/s), representing an electrical load on the generator), as the flywheel inertia is increased, the power quality is improved, and the maximum torque increases. When increasing the flywheel inertia by a factor of 3, the power quality is improved by a factor of 1,7 and the torque is increased by a factor of 2,6. (*Note that a lower numerical value of power quality denotes smoother power output. A power quality value of 1 denotes completely smooth power output.)*

At a higher damping coefficient (20 N*m/(rad/s)), an equivalent increase in flywheel inertia has a lesser impact on the power quality, with a reduction of a factor of 1,4 whilst the maximum torque increases by a factor of 3,3 and the torque on the generator doubles. With a doubling of the signal gain, these gains in power quality remain the same, whilst the torque doubles. The signal gain represents the input signal amplitude; a value of 1,3 is the nominal signal, i.e. the signal is as close as is possibly to the real data recorded from the Tordenskiold when at sea (see annex, figure 24). A doubling of the signal gain to 2,6 represents a doubling in the amplitude of the signal (i.e. a doubling of wave height), but it does not change the wave-length or any other attributes of the input signal.

Flywheel Inertia (kg*m^2)	**Signal Gain**	**Peak Rack Velocity** (m/s)	**Damping coefficient** (N*m/(rad/s))	**Power Quality**	**Peak Torque** (Nm)		
					Before gear	After gear	At generator
8.4	1.3	0.49	10	13.2	5129	941	213
16.8	1.3	0.49	10	9.7	7402	1370	213
25.2	1.3	0.49	10	7.8	13120	2435	213
8.4	2.6	0.97	10	13.2	10258	1882	426
16.8	2.6	0.97	10	9.7	14800	2740	426
25.2	2.6	0.97	10	7.8	26420	4869	426
8.4	1.3	0.49	20	15.5	3959	726	426
16.8	1.3	0.49	20	13.2	6300	1166	426
25.2	1.3	0.49	20	11.2	12940	2402	426
8.4	2.6	0.97	20	15.5	7918	1453	852
16.8	2.6	0.97	20	13.2	12600	2332	852
25.2	2.6	0.97	20	11.2	25880	4803	852

Table 1. Results of simulation of Tordenskiold with low, mid, and high inertia flywheels (coloured horizontal lines), two wave amplitudes (denoted by the signal gain), and two different damping coefficients (simulating electrical loads). The signal input is real data recorded from the Tordenskiold. Note that a lower value of power quality denotes smoother power output.

1.5.2.4. Evaluation

It is clear that the addition of mass, and thereby inertia, to the flywheel has a positive effect on power smoothing. Naturally it has an influence on the torque transmitted through the PTO, with the torque increasing significantly with the addition of flywheel inertia.

These results also demonstrate the challenge in choosing the correct flywheel inertia for variable sea-states. As the amplitude of the wave is increased, the torque increases disproportionally to the improvement in power quality.

This model can be greatly improved upon by comparing the outputs to reliable real data collected from the Tordenskiold when they become available.

1.5.3. Modelling of a Power-Splitting Device

1.5.3.1. Introduction

Power smoothing with the use of a flywheel can be further improved with the use of a power-splitting mechanism, such as a planetary gear. Similar systems have been employed on 'The Ocean Harvester', a point-absorber type of WEC that utilizes power splitting to distribute mechanical power between the generator shaft and a suspended mass (Josefsson, 2016). While an offshore suspended mass is not practical in the case of the Crestwing WEC, an additional flywheel serves the same function. They have also been proposed for use in hybrid electric vehicles, replacing the need for batteries. They are lighter, less expensive, have a greater rate of energy storage and return with lower losses, have a much greater lifespan, and their production is less damaging to the environment (Su, 2010).

1.5.3.2. Method

A Simulink model was constructed using the same underlying components, damping, and dimensioning as the previous example, only the power from the shaft directly before the generator and flywheel was split using a planetary gear.

A 2:1 ring to sun gear ratio was employed, dividing the power between two shafts; the higher speed ring gear shaft was attached to a low-inertia flywheel (5 $kg*m^2$), whilst the lower speed sun gear was coupled to the generator with a high-inertia flywheel attached (16 $kg*m^2$).

To control the relative speed of the two shafts, a hydraulically actuated disk friction clutch was placed between the shafts and on the generator shaft, allowing the regulation of the power transmitted to each shaft. The hydraulic actuators are controlled by a PID controller, which limits the rotational velocity of the generator shaft to a predetermined value. Before this value is reached, all available power is transmitted to

the generator shaft. Once this value has been reached, any additional power from the wave is distributed between the two shafts with just enough passed to the generator to maintain its rotational velocity, and any excess power being stored in the increasing rotational velocity of the high-speed flywheel shaft. Finally, when the wave can no longer provide enough torque to maintain the generator speed, the high-speed flywheel returns its stored power to the generator shaft, maintaining its speed and torque until the next wave arrives.

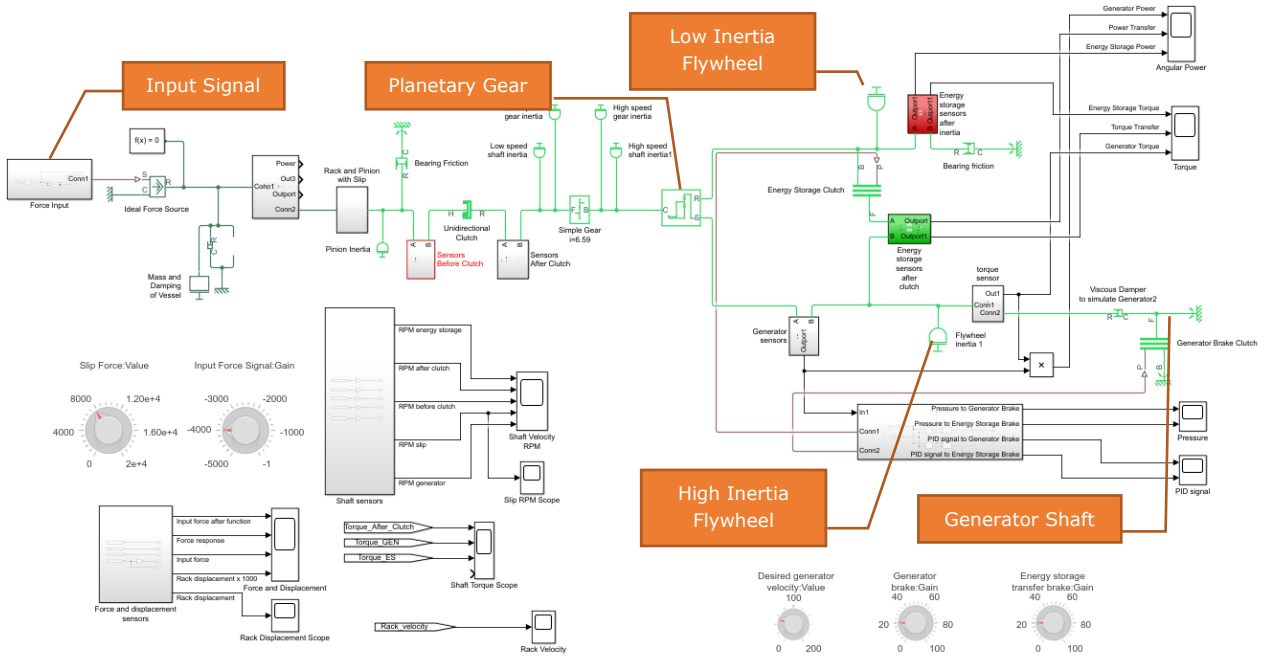

Figure 16. Block diagram of a Simulink model that splits the incoming power between two shafts in order to store power in a high-speed flywheel and return it to the generator shaft when required.

1.5.3.3. Results

This model was run for 200 seconds, with the final 100 s graphed below. What is clear from this simulation is that a constant power output can be achieved in an entirely mechanical way using flywheels as a form of short-term storage. With adaptive PID control, the power output of the generator can be tuned to the sea-state, i.e. a higher power output can be maintained when there is more wave energy available.

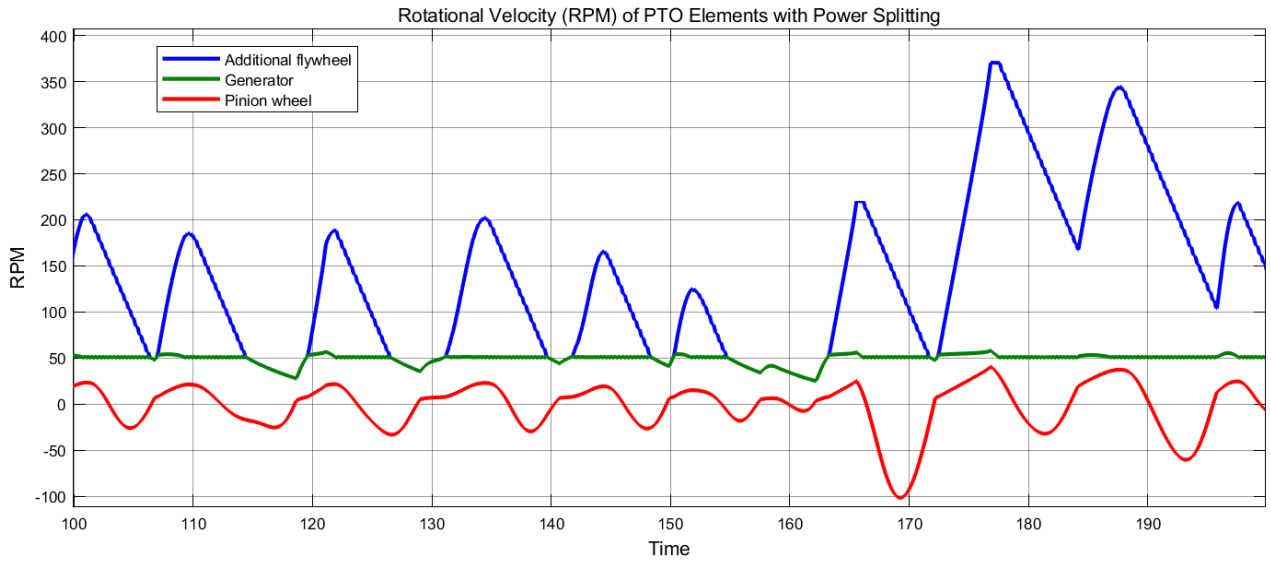

Figure 17. Graphical output of a Simulink simulation whereby incoming mechanical power is split between a low speed, high inertia flywheel, and a high speed, low inertia flywheel. The blue, green and red lines represent the high inertia ('additional flywheel'), low inertia ('generator'), and shaft input ('pinion wheel') RPM respectively.

In the example in figure 17 above, the generator speed has been set to 50 RPM (green line), as this speed can be maintained in the relatively small seas simulated. The additional flywheel stores mechanical power as kinetic energy as it is sped up beyond the 50 RPM of the generator. As each wave passes and the pinion wheel slows and reverses direction (red line), the stored energy is passed to the generator shaft. In this particular example, generator speed dips below the 50 RPM on occasion as the power stored in the additional flywheel is exhausted, i.e. the RPM of the generator power output is set slightly higher than can be maintained under the sea state simulated. This results in a power quality of 1,4. However, the power quality can in principle be reduced to 1, whereby the peak and the mean power outputs are the same, i.e. a perfectly smooth power output.

1.5.3.4. Evaluation

This method does present some serious engineering challenges, mainly in terms of the wear that would be expected on such a mechanism, and its complexity. It also faces a similar problem to that of the simple flywheel in that the rotational inertias of the flywheels are fixed, and must be carefully dimensioned for the prevailing sea state to avoid power losses though torque protection, especially when considering long-period open-ocean swells. However, by adjusting the electrical load and rotational velocity constraints placed on the generator, this system can deal with a broader range of sea states than a simple flywheel, and it can greatly reduce the need for further power smoothing, in principle to the point where no further short-term smoothing is required.

1.5.4. Modelling of the Array Effect

1.5.4.1. Introduction

One of the most significant challenges of ocean waves as a source of renewable energy is the large peak-to-average power ratio. This ratio determines the power quality, and must be reduced through the chain of power collection to supply. One of the more costly aspects of WEC components is their need to accommodate the greatest peaks of power input whilst efficiently operating at a lower power level. Active components and control methods can be complex, costly, and require maintenance - therefore, any passive methods of improving power quality must be prioritised.

The fact that the Crestwing WEC would ultimately be grouped as a farm introduces an important passive power smoothing and optimization effect; that of array power smoothing. Experiments with the array configuration of the 'Lifesaver' point-absorber, found that the natural smoothing effect of having multiple connected WECs reduced the peak-to-average power ratio by a factor of 3-5 (Sjolte, 2013). This is illustrated in figure 18, below, whereby a simple half sine wave (with negative values removed to simulate the effect of the one-way clutch) is duplicated with a short time delay. This simulates a simplified group of five vessels responding to the passage of a wave, with the wave striking each vessel at a slightly different time. When the sine waves are added, the resultant output is a relatively smooth signal, which does not drop to zero (the dashed red line, figure 18).

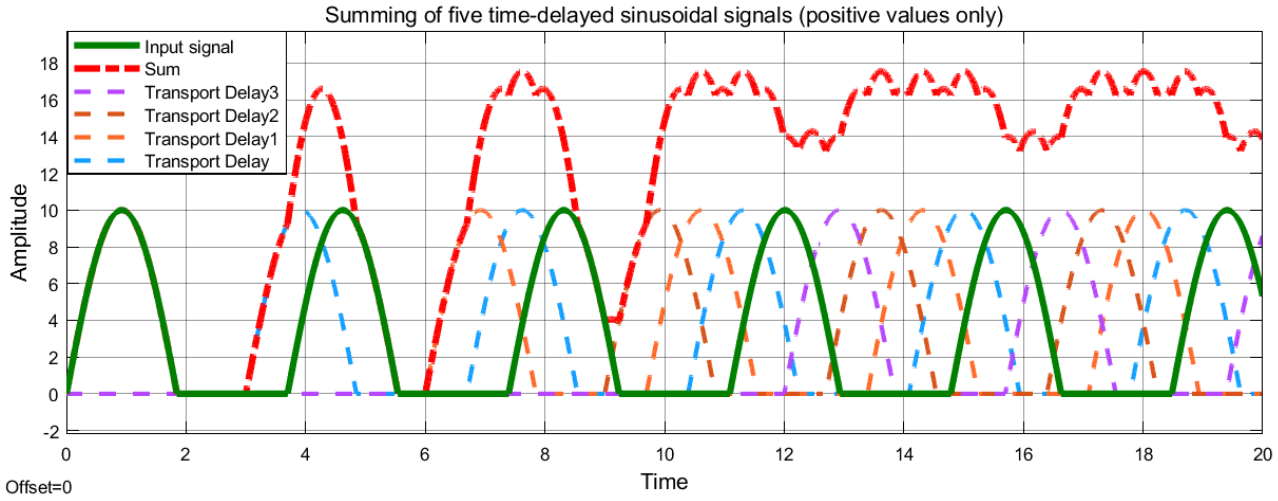

Figure 18. Effect of adding five time-delayed sinusoidal waves, with the negative values removed. The green line represents the input signal, which is duplicated four times, each time with a delay ('transport delay'). These signals are summed to create the red line ('sum') which maintains a relatively stable higher value, and does not drop to zero.

Ruiz *et al.* (2017) describes a mathematical means of optimizing the layout design of WEC arrays based upon either a fixed number of vessels, or a fixed area in which they are to be deployed. This can be used to

maximise the power output and minimise the vessel interference, although the results of their study highlights the complexity of the optimisation problem. In future studies, when the precise design, number, and location of the Crestwing vessels has been determined, it would be useful to investigate this further, but with so many unknown variables at play, it would not be a meaningful exercise for this study.

However, the impact of vessel placement and number in relation to power smoothing is of great concern at this point in the design process, as its inclusion has a significant impact on the requirements of the vessels' PTO and electrical components, including cabling.

1.5.4.2. Method

The array effect was simulated for the Crestwing WEC, based upon real data from the generator output of the Tordenskiold on March 21st 2019. This model serves to illustrate the natural smoothing effect, based only on the time-delay of power output caused by the regular spacing of vessels.

The simulation was run for 1250 seconds, and used a transfer function to improve the quality of the input graph (due to low data fidelity). Missing data was approximated using the mean of the neighbouring values, and the signal transport delay was set between 6,0 and 10,5 seconds. These delays were incrementally summed to create a total delay of the final signal of 72.5 seconds. The final 5000 data points were logged, avoiding the initial simulation period where not all the signals were running.

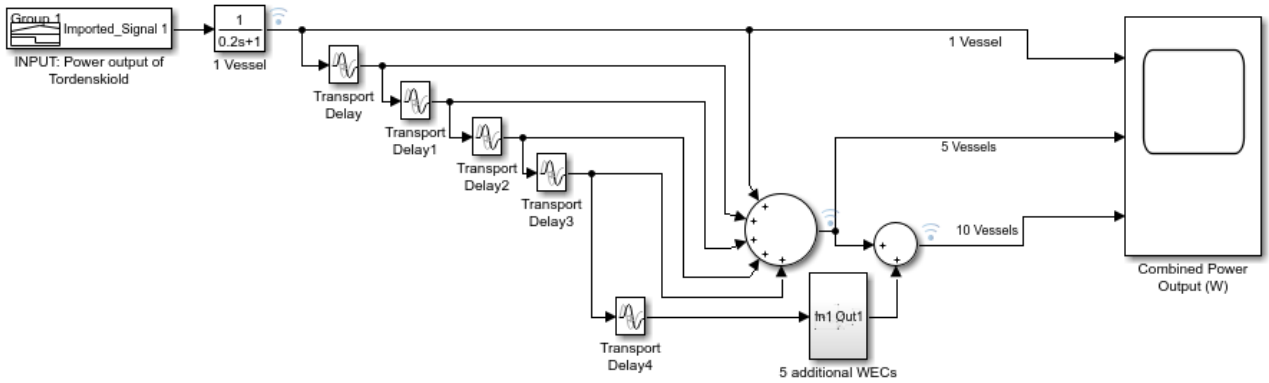

Figure 19. Block diagram of Simulink model. The real electrical power output data recorded from the Tordenskiold on March 21st 2019 is used as a signal input (far left of model). This input signal is smoothed using a transfer function and duplicated. With each duplication a time delay is introduced. The signals are then summed as a combined power output (far right).

1.5.4.3. Results

The graph below illustrates the impact of the addition of power output with a time delay of between 6 and 10,5 seconds, with the blue, orange and green lines indicating the combined power output of 1, 5, and 10

vessels respectively. Whilst the peak power output is clearly higher as more vessels are added, the peak-to-mean is significantly reduced, i.e. the power quality is improved (see table below).

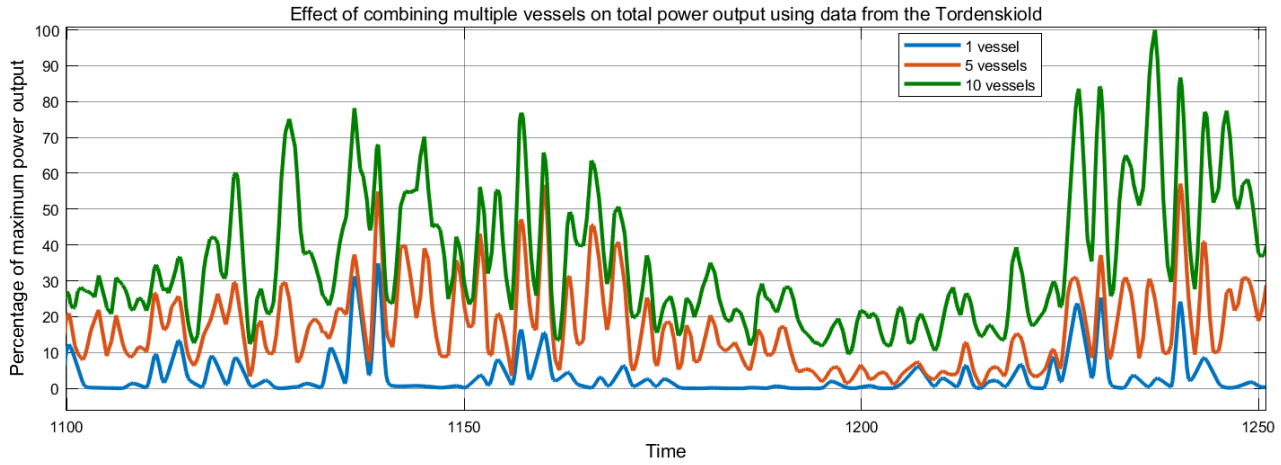

Figure 20. 150 second sample of a Simulink simulation illustrating the power output of the Tordenskiold (blue), and a combination of identical time-delayed signals, representing an array of five (orange) and ten (green) vessels.

No. of Vessels	Power Quality
1	12.4
5	4.8
10	2.8

Table 2. Numerical results of the last 5000 logged points (approx. 1050 seconds) of a Simulink simulation of time-delayed summed power outputs of the Tordenskiold. A lower power ratio represents a higher power quality.

Note that the power ratio drops from 12.4 to 2.8 with one and ten connected vessels respectively. This is an improvement in power quality by a factor of four, with no mechanical or electrical power storage.

The array method does, however, have its limitations. In order for power cables to be joined together and the power summed, the power must be conditioned in one of two ways; either the AC output from the generators must be matched, or the AC must be converted to DC, and then controlled to a set output voltage. If low voltage DC is selected, then limits are placed on the size of the array due to the current that may be carried by sea cables; a maximum of 1000 A per cable is considered to be a practical limit (Sjolte, 2013).

1.5.4.4. Evaluation

The results of the array simulation suggest that the power quality of the Tordenskiold can be vastly improved by considering a number of physically offset vessels in an array and joining their power output. This

improvement in power quality is entirely passive and therefore requires no additional hardware - just a carefully considered optimization of the number and placement of the vessels.

1.5.5. Other Power Transmission and Power Smoothing Methods

1.5.5.1. Introduction

So far, only flywheels, mechanical power-splitting, and passive power-smoothing methods have been considered. However, there are many other possibilities for the partial or complete smoothing of power, both off-shore and on-shore. These are briefly considered here.

1.5.5.2. Mechanical Power Smoothing; Variable Inertia Flywheels

Aside from the power splitting and flywheel methods already explored, another potential method of power smoothing is through the use of a **variable inertia flywheel**. Variable inertia flywheels are capable of changing the distribution of their mass, and therefore their rotational inertia, either actively (with some sort of control system) or passively (with springs).

When investigating their use in hybrid electric vehicles, Su *et al* (2010) found that such systems were best suited to heavy vehicles that would stop and go with severe acceleration and deceleration. Their use was found to significantly improve energy efficiency, besting all other methods tested.

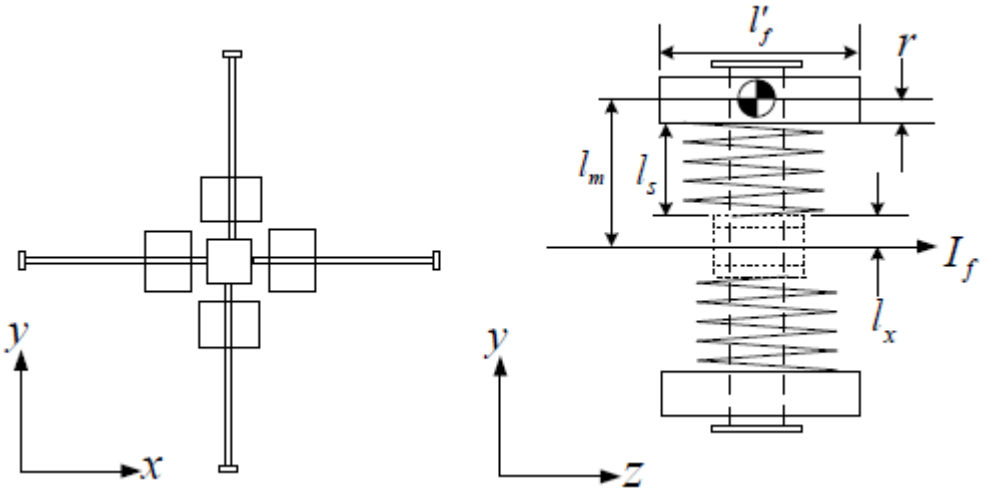

Figure 21. Design possibility for a variable inertia flywheel. Reproduced from Su (2010).

This method would be well suited for use in the Crestwing PTO, especially when considering a passive version of this mechanism, as it would allow the transmission of unregulated torque to the generator and flywheel, whilst allowing for an increasing storage of power (in the form of kinetic energy) with an increasing degree

of power input to the PTO. In short, if correctly designed, it would be capable of smoothing individual waves to some extent, whilst also being able to adapt to changing sea conditions.

1.5.5.3. Electrical Power Smoothing; Super Capacitors

Super capacitors are an increasingly attractive alternative to battery storage as their cost steadily falls with time. They have many useful characteristics, including;

- A high power density
- Rapid complete discharge (seconds) due to the charge being stored in electrodes
- Compact size
- A relatively long cycle-life expectancy, reaching more than 500,000 cycles.

However super capacitors are only useful for controlling power fluctuations over short periods of time, since they have a large self-discharge rate.

1.5.5.4. Evaluation

With increasing complexity in a harsh offshore environment, comes an increasing cost of installation, and an increasing risk of breakdowns and costly maintenance. Therefore, simple, passive, inexpensive, and proven components are preferred for power transmission and smoothing. Additionally, onshore components are preferred to offshore for the same reasons.

It is anticipated that the final plan for a full-scale Crestwing wave farm will involve multiple vessels linked together, and therefore the passive smoothing of power using the array effect will be an important factor in power smoothing. This will reduce the necessity for some costly power smoothing and conditioning components, although an absence of any power smoothing from the start of the power train leads to the need for the over-dimensioning of components to cover the large mean-to-peak power fluctuations. This over-dimensioning is transmitted through the power train unless dealt with as close to the source as possible. Therefore, a balance must be found between power smoothing at, or close to, the power source, with the associated costs and complexities, and power smoothing at subsequent stages of the transmission train.

Whilst complete power smoothing is not necessary, the results of this study suggest a simple flywheel is not sufficient to meet the variable wave-states that the Crestwing WEC is expected to operate under. Therefore, a passive variable inertia flywheel is recommended for serious consideration as an alternative. Additionally, whilst it is anticipated that electrical storage will be required at the final stage of power transmission, further expertise in offshore high-voltage electrical engineering is required to make a fully informed decision as to the best approach.

1.5.6. Realisation of Project Objectives

This project has met the project objectives 1, 2, and 3, i.e. an analysis of the data collected from the Tordenskiold, an analysis of the possibilities for power smoothing, and the construction and analysis of a mathematical simulation of the Tordenskiold PTO.

However, there were unexpected difficulties in obtaining high-quality data from the Tordenskiold with which to match the mathematical model to. These difficulties (described in section 1.4) meant that objective 4 was only partially met, as the mathematical models could not be used to predict the maximum output of the Tordenskiold, and thereby the required generator dimensioning.

The inability to reliably match the models to the data recorded from Tordenskiold, and the lack of clear trends in those data (in terms of the PTO's response to changes in electrical load), meant that a complete economic assessment of the optimum PTO set-up could not be made, and therefore objective 5 could not be met. However, this project did investigate the need to consider the power conditioning and transmission costs, from the offshore source to grid, and the importance of integrating these elements into the Crestwing design at the earliest stage of development.

These results are important in highlighting the need for further investigation into the correct dimensioning of the generator in order to maximise the potential power output of the Tordenskiold and subsequent full-scale vessels. It is expected that onshore testing of the Tordenskiold PTO will begin Autumn 2019, and the models developed for this project will be refined with the anticipated availability of high-quality data. These models will then be available to be used for further testing of the addition of simple flywheel masses, and other more significant changes to the PTO.

There will also be further investigations into the potential of using variable inertia flywheels, to maximise the power output potential of the Crestwing, whilst minimising the shaft torque, and associated wear.

This project also highlighted the significant discrepancies in the real data recorded from the Tordenskiold, and the data that should reasonably be expected. The Simulink models aided in the realisation of these discrepancies, and following investigations are to be made:

- The load cells on the Tordenskiold's PTO rod are to be examined and re-calibrated.
- High frequency data is to be made available for, at minimum, the rod load, rack displacement, and generator RPM.

- The Tordenskiold's PTO components are to be checked for unusual wear and resistance to motion.
- An additional one-way clutch is to be installed between the gear and the flywheel and generator. This is to prevent mechanical losses as currently the flywheel must drive both the generator and the gears when in free-wheel.

The possibilities of adding an electro-magnetic or mechanical brake are being investigated, with the aim of adding much greater mechanical resistance to the rotation of the PTO shaft than the currently installed generator and electrical resistive loads can provide. This is to further investigate the maximum power output potential of the Tordenskiold without investing in costly generators

1.5.7. Dissemination of Results

These project results were disseminated at a Crestwing project planning meeting on July 1st 2019. Here the results were explained and discussed, and a plan for the future of the Crestwing PTO development was formulated.

Some of the results have been published in the Professional journals Ing.dk and gridtech.dk

- Date 12.06.2019

  There was an article with the name "Efter fem måneders test: Bølgerne rummer endnu mere energi end generatoren kan omdanne." on the net news www.ing.dk.
- Date 13.06.2019

  The same article was on www.gridtech.dk
- Date 28.06.2019

  In the summer special newspaper (only on the net) www.ing.dk had an article with the name "Hængslede vinger høster bølgekraft.". Here Ingeniøren received some graphics from Crestwing and put it nicely together.

This document (or an appended version) will also be further disseminated amongst those involved in the Crestwing project.

1.6. Utilization of Project Results

The results obtained in this project "Development of Crestwing's Power Take Off system" has given Crestwing great information about the PTO system, the data quality, and its collection. Furthermore, it has pointed out the next focus points and development.

The original project partners that participated in 2013 are, for different reasons no longer participating. However, Crestwing has partnered with a strong technical group consisting of companies and individuals who have strived in the past years to realize the Crestwing concept that Henning Pilgaard invented and developed over 12 years, and which we believe to be a competent participant in the wave energy field. Also, energinet.dk, that supported Henning Pilgaard for ten years, had expectations to the fulfilment of the concept.

Crestwing has planned to test Tordenskiold in Autumn 2019 with the changes we will have applied from the results from this present test period.

When the modifications and new test period are completed, and we are satisfied with the results, we will begin to seek grants and investors to engineer and build a full-scale device for the North Sea.

We have high expectations for the commercialization of the Crestwing concept after the successful tests with Tordenskiold this past winter.

The market potential for wave energy is enormous, as most of the world's governments have decided that we shall turn away from fossil fuels. The earth consists of two-thirds ocean and one third land. There is around 7,7 billion people on the planet, growing to 9 billion in 2050. The amount of renewable installations required to meet the demand of green power supply are enormous, and there are great challenges to meeting this demand on land, especially on land where people live and near the coast.

There still does not exist anywhere in the world a wave energy converter capable of producing profitable energy, which is a disaster for the pace of the transition of the energy supply from black to green. Although many attempts have been made, there is still not a concept comparable to the three bladed wind turbine. Hereby we say that the market for wave energy is enormous and there are no competitors that have made a breakthrough.

This, the EU has acknowledged, and has started new programs, e.g. OESA northsearegion.eu/oesa/, to promote wave energy.

Crestwing has patented the manner of harvesting energy from the ocean and is considering protecting our rights further by taking out more patents, or by going public, or by employing a “Brugsmodel” on the PTO system and the mooring system.

1.7. Project Conclusion and Perspective

This report has made significant progress towards the development of a PTO system capable of delivering electrical power to the national grid. It has identified the advantages and disadvantages of increasing the flywheel inertia to smooth power output, and has investigated a method for completely smoothing the power output from the Tordenskiold using mechanical means. Significantly, it has identified the need to take into consideration the impact of linking two or more vessels together in terms of passive power smoothing, and the need for careful consideration of the power conditioning and transmission architecture at a very early stage of the design process.

The conclusions of this report are as follows:

- An increase in the mass of a simple flywheel serves to enhance power smoothing, but at the cost of increased torque on the PTO shaft. Whilst a flywheel can be optimized to a specific sea-state, its effectiveness diminishes outside of this optimized state. With the addition of a torque limiter, a simple flywheel can operate under higher than optimal sea-states, but will waste potential power and be subject to wear. Without a torque limiter, at higher than optimal sea-states the power smoothing will be reduced, and the PTO shaft may be exposed to excessive torque.

- Simulink models demonstrate the possibility of using an active mechanical method to split power between two flywheels of different fixed inertia, thus allowing the complete smoothing of power at the source. However, this adds cost and complexity to the PTO.

- Further Simulink modelling of the array effect (using real data from the Tordenskiold) indicate that complete power smoothing is not necessary at the PTO, as the effects of simply adding the power output from several vessels can improve the power quality (mean-to-peak mechanical power output) from 12,4 to 2,8 (one and ten vessels respectively).

- If linking multiple vessels, some power smoothing within the PTO might be advantageous to limit downstream over-dimensioning of components. Passive variable-inertia flywheels are good candidates for this purpose and warrant further investigation.

- A power conditioning and transmission architecture is recommended to take advantage of the passive power-smoothing effects of multiple connected vessels. This could consist of an AC/DC/DC/AC arrangement if connecting to an onshore electrical grid, possibly with the aid of super-capacitors for the final stage of power smoothing.

- In reference to the data downloaded from the sensors on-board the Tordenskiold, it is clear that there are discrepancies in the data from one period of time to another. Furthermore, it appears that the data from the rod load-cell is suspect, and requires further investigation and possible recalibration. In addition, it is clear that the low-frequency data is insufficient for use as a reference point from which to calibrate the simulations.

- Improvements to the freewheeling of the generator a flywheel can be improved by placing a one-way clutch between the gear and the generator of the PTO. This will prevent the flywheel from having to provide energy to turn the gears as well as the generator when in free-wheel.

- The rectifier and capacitors can be removed from the power conditioning system on-board the Tordenskiold, instead coupling the dumploads directly to the generator. A Maximum Power Point (MPP) must also be added.

- The addition of a brake to the PTO is worth serious consideration, as this would allow a calculation of the maximum power output that the Tordenskiold is capable of, without investing in additional generators and dumploads.

- Calibration of load cells and load pins must be performed. Measurements should be made before and after calibration.

- The Tordenskiold PTO should be tested when docked in Frederikshavn harbour. The motion of the PTO can be simulated with the use of an electric or hydraulic motor.

- The PTO sensors should be tested and high-quality data (5 Hz or above) captured from the most relevant components. These will be used to further improve the mathematical models of the Tordenskiold.

Month	July				August				September		
Week	29	30	31	32	33	34	35	36	37	38	39
Repair and Modification of PTO (VMS/CW)											
Check-up of pneumatic and slip couplings											
New freewheel coupling between gear and generator											
New sleds on the rack											
New longer push-rod											
Possible extension of slide-bars											
Possible installation of a brake											
Miscellaneous (CW)											
Ventilation											
Sealing balls											
Seal housing											
Electronics (ES/SC)											
Repair of burned-out contacts in the electronics cabinet											
Change of generators attachment to batteries and dumpload											
RPM to the flywheel											
Camera											
Programming (SPICA, ES, SC)											
Programming of MPP function											
Wave-measuring equipment											
Calibration of sensors											
Onshore (CW/Vetec/VMS)											
Repair of dents and other damage											
Check, removal, repair and reinstallation of load pins											
Painting											
Testing (VMS/ES eftf/SC/CW/NIRAS/SDT)											
Set-up of PTO onshore with hydraulic actuator											
Testing											
Launch											
Check the anchorage with divers											
Launch and positioning of wave-measuring equipment											
Launch and positioning of Tordenskiold											

Table 3. Summer/Autumn 2019 schedule for programme development.

List of Figures

List of Tables

References

Josefsson, A., Berghuvud, A., Ahlin, K., Broman, G., 2011. 'Performance of a Wave Energy Converter with Mechanical Energy Smoothing'. European Wave and Tidal Energy Conference, 2011.

Ruiz, P., Nava, V., Topper, M., Minguela, P., Ferri, F., Kofoed, J., 2017. 'Layout Optimisation of Wave Energy Converter Arrays'. Energies 10, 1262.

Sjolte, J., Tjensvoll, G., Molinas, M., 2013. 'Power Collection from Wave Energy Farms'. Applied Sciences 3, 420–436.

Su, H.-K., Liu, T., 2010. 'Design and Analysis of Hybrid Power Systems with Variable Inertia Flywheel'. World Electric Vehicle Journal 4, 452–459.

Annex

A. Description of Simulink Model of Tordenskiold PTO

The Simulink model of the Tordenskiold is laid out below, with each numbered section described in detail.

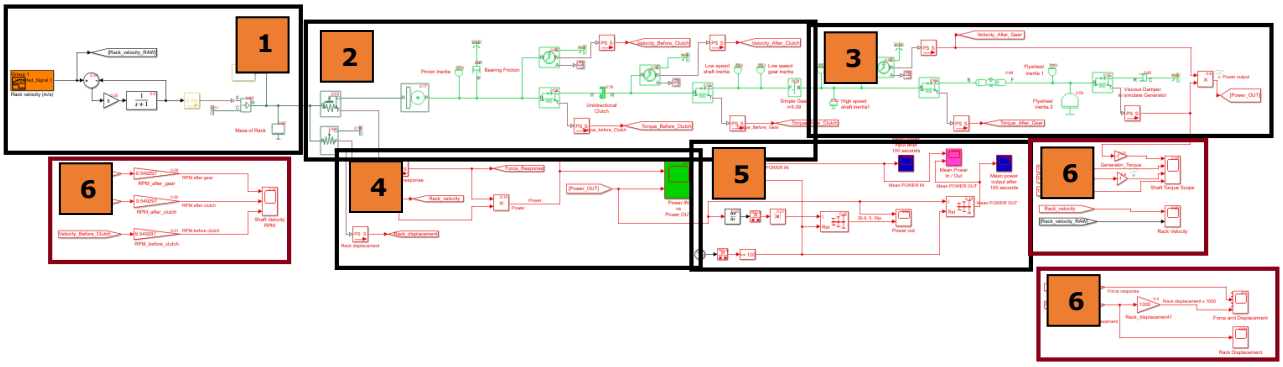

Figure 22. Overview of the Tordenskiold Simulink model. The model is divided into sections which are explained further below.

A.1. Section 1

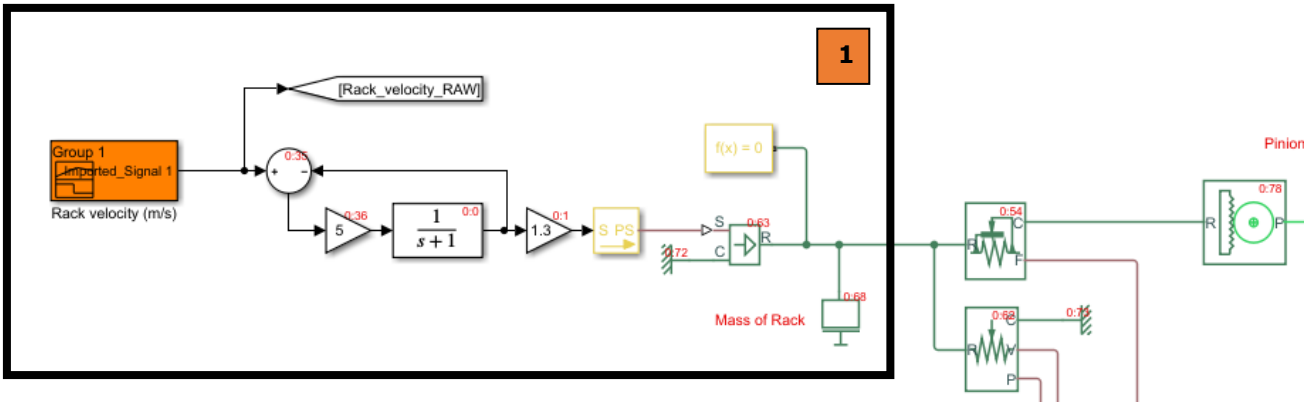

Figure 23. Section 1 of the Tordenskiold Simulink model; From signal input and modification (left) to the PTO rack (right).

Here, the real rack velocity data from the Tordenskiold is used as a signal input. This is calculated from the change in rack displacement as a function of time. This passes through a transfer function (to smooth the raw data to a more usable signal – see figure below), and a 'Gain' block, which multiplies the output by 1,3 to better match the smoothed signal to the original. This signal then passes through a Simulink 'Signal to Physical Signal' block and on to an 'Ideal Velocity Source' block. This is grounded at the 'C' input, and the linear velocity of the rack is transferred to the next section. Also connected is a mass block, representing the mass of the rack, a solver block, and a 'Goto' block, which sends the signal to a corresponding 'From' block elsewhere in the model.

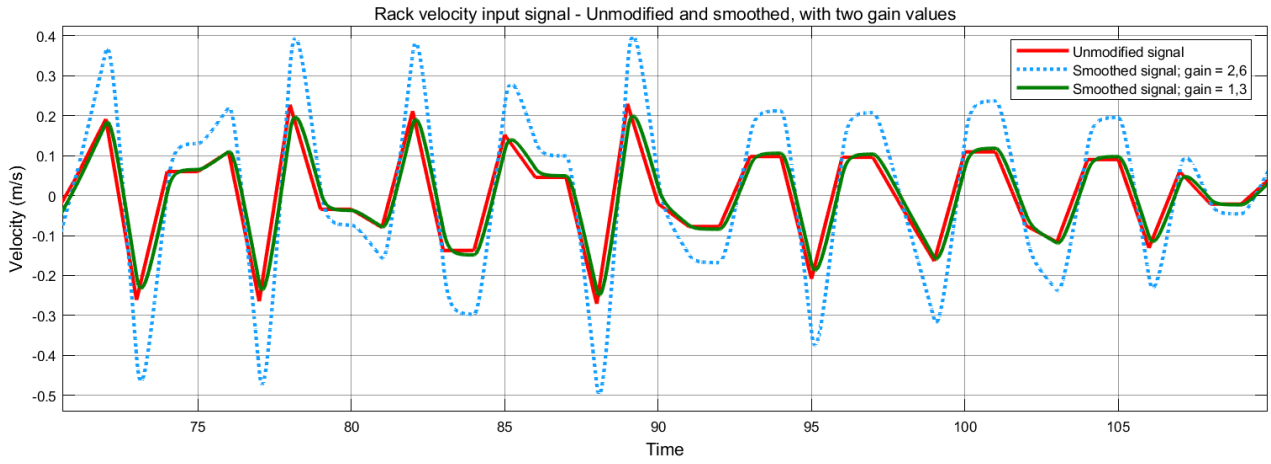

Figure 24. A 40 second graphical display of the rack velocity input signal (m/s) comparing the unmodified (red) and modified signals with a gain of 1,3 (green) and 2,6 (dotted blue).

A.2. Section 2

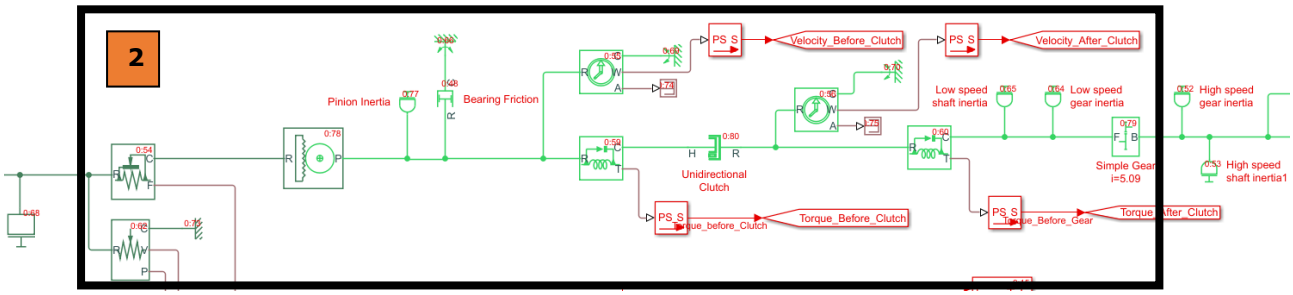

Figure 25. Section 2 of the Simulink model. From the rack and pinion (transition from dark to light green, left) to the step-up gear (right).

This next section considers the physical components of the PTO from the rack to the gear. From left to right are the following components:

- 'Ideal force sensor' – *this measures the linear force applied on the rack.*
- *Below this, an* 'Ideal motion sensor' – *this measures the rack travel and velocity.*
- 'Rack and Pinion' – *this transforms the linear motion to rotational motion. The size of the pinion wheel is manually input.*
- 'Inertia block' – *this represents the rotational inertia of the pinion wheel. This, and all other inertia values were calculated using the CAD drawings of the PTO system supplied by Crestwing.*
- 'Rotational damping' – *this represents bearing friction in the pinion.*
- 'Ideal motion sensor' – *this measures the rotational velocity of the PTO.*
- *Below this, an* 'Ideal torque sensor'.
- 'Unidirectional clutch' – *this allows rotational motion in only one direction and offers no resistance to motion in the opposing direction.*
- 'Ideal motion sensor'.
- 'Ideal torque sensor'.

- 'Inertia block' – *this represents the rotational inertia of the low-speed shaft.*
- 'Inertia block' – *this represents the rotational inertia of the low-speed gear-box.*
- 'Simple gear block' – *this represents a simple gear with an adjustable gear ratio (i=5,09).*
- *Also included are four* 'PS-S' *blocks (physical signal to signal), and their corresponding Goto blocks.*

A.3. Section 3

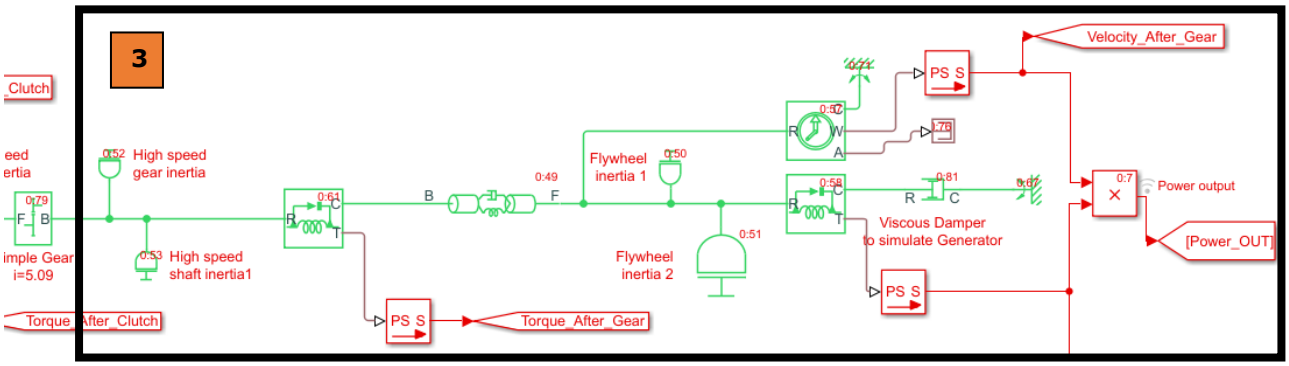

Figure 26. Section three of the Simulink model. From the high-speed axel after the gear (left) to the viscous damper (simulating the generator) and power output calculator (right).

The next section continues the physical components of the PTO system from the gear to the generator:

- 'Inertia block' – *this represents the rotational inertia of the high-speed gear-box.*
- 'Inertia block' – *this represents the rotational inertia of the high-speed shaft.*
- 'Ideal torque sensor'.
- 'Flexible shaft' – *this represents a flexible coupling and limits spikes in torque transferred to the subsequent components of the PTO.*
- 'Inertia block' – *this represents the flywheel currently installed on the Tordenskiold.*
- 'Inertia block' – *this represents additional flywheel inertia for testing.*
- 'Ideal motion sensor'.
- 'Ideal torque sensor'.
- 'Viscous damper' – *this represent the generator load. It is an ideal mechanical rotational damper, with an adjustable damping coefficient. This can be adjusted to match the model to the real data.*
- 'Product block' – *this multiplies the rotational velocity and the torque to calculate the mechanical power. This product is attached to the 'Power_OUT'* 'Goto' *block.*
- *Also included are three* 'PS-S' *blocks (physical signal to signal), and their corresponding* 'Goto' *blocks.*

A.4. Section 4

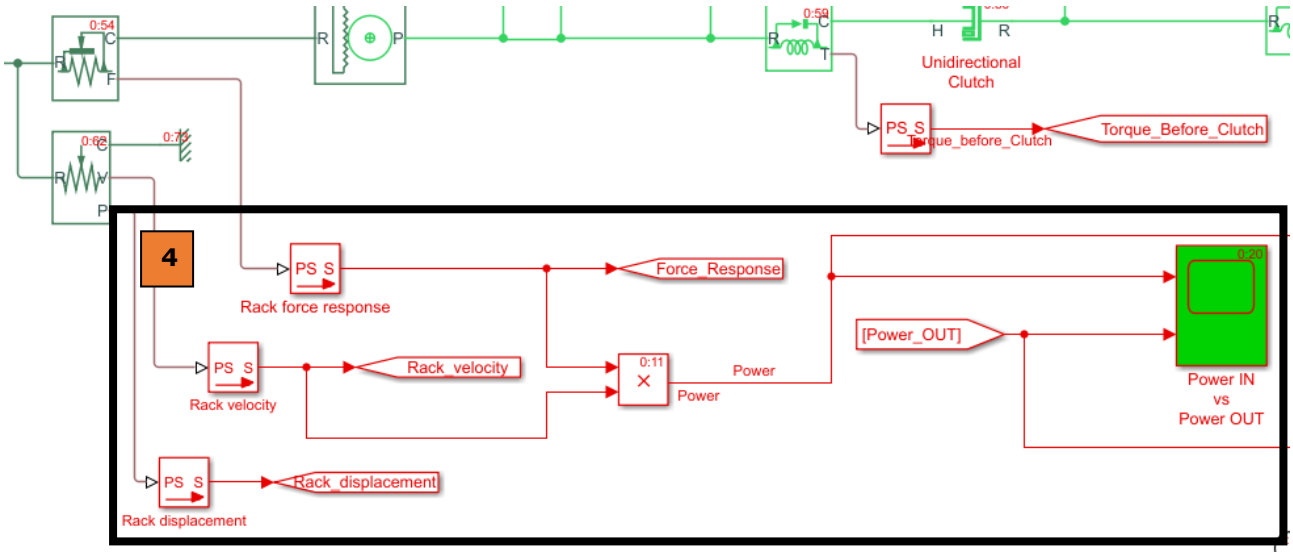

Figure 27. Section four of the Simulink model. The input power calculations and visualisation scope.

This section simply takes signals from the ideal force and movement sensors attached to the rack, and sends them to corresponding 'Goto' blocks. Here the product of linear force and velocity is calculated to provide the mechanical power that is input to the PTO. The green 'Scope' block, named 'Power In vs Power OUT' is used to visualise the mechanical power signals calculated here and in the previous section.

A.5. Section 5

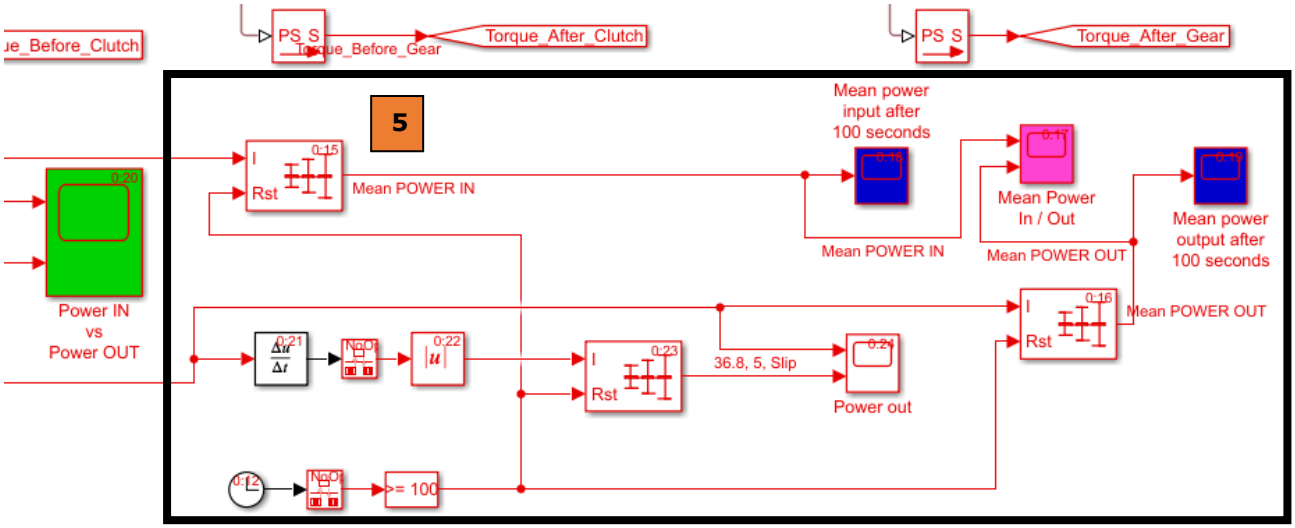

Figure 28. Section five of the Simulink model. The calculation of running mean values of power.

This section simply deals with calculating the mean mechanical power output and input over each 100 second period that the simulation is run. It utilises Simulink 'Running Mean' blocks which mask the underlying mathematic model.

A.6. Sections 6

The three section 6's are simply the 'From' blocks that correspond to the previously described 'Goto' blocks, and 'Scopes' for visualization of the signals.

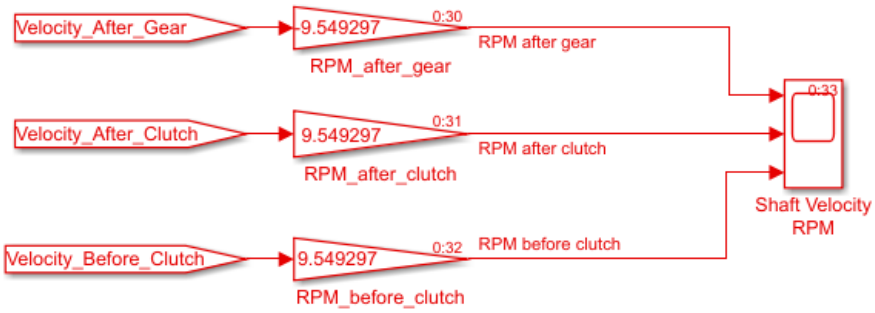

Figure 29. Section six of the Simulink model: The 'From' blocks relating to rotational velocity at three points in the PTO. The signals pass through 'Gain' blocks which multiply the signal by 9,549297. This value converts radians to RPM.

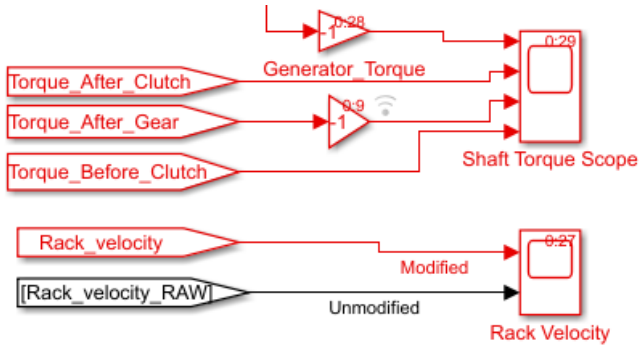

Figure 30. Section six of the Simulink model: The 'From' blocks relating to torque and rack linear velocity signals. Two torque signals pass through a 'Gain' block set to -1. This simply converts the negative torque values to positive, allowing for easier visualization of the signals.

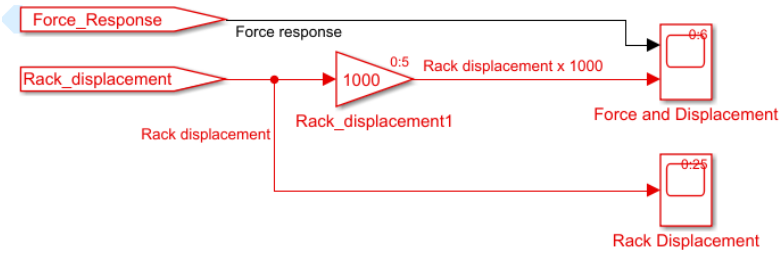

Figure 31. Section six of the Simulink model: The 'From' blocks relating to rack displacement and the force response of the PTO to the input velocity signal. The rack displacement signal is split into two, with one copy passing through a 'Gain' block set to 1000. This is to allow visualization of the force and displacement on one graph.

B. Description of Simulink Model of Power-Splitting

The Simulink model of the proposed power-splitting PTO is laid out below, with each numbered section described in detail.

B.1. Sections 1 & 2

The model has the same input structure as the previous model (Annex A), and sections 1 and 2 (annex A1 and A2 respectively) are exactly the same, and therefore excluded from the figure below.

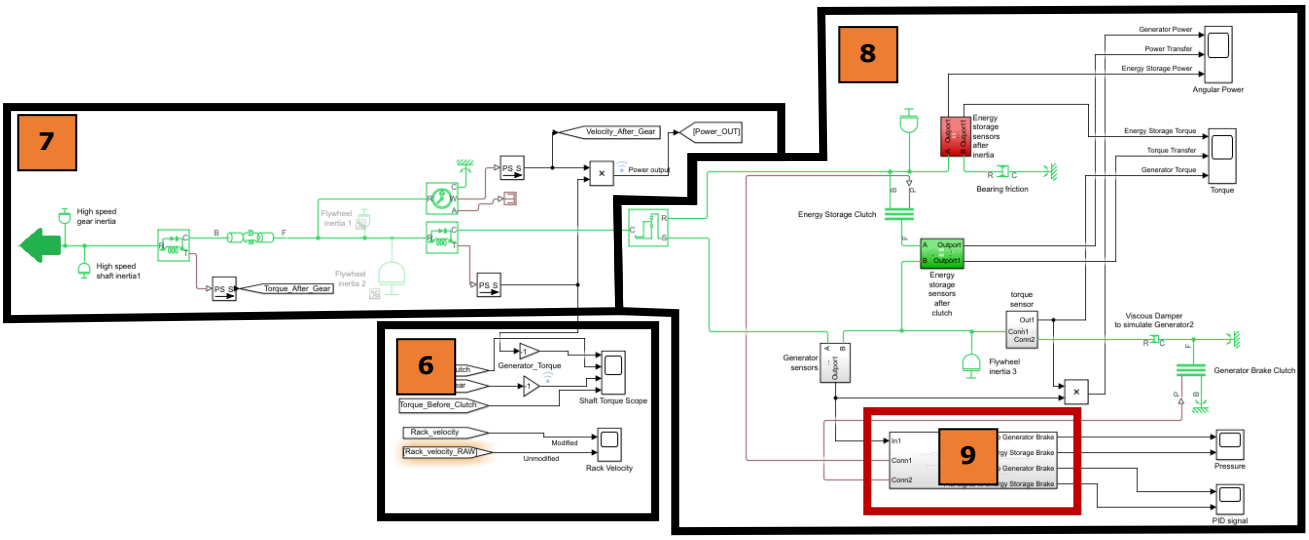

Figure 32. Overview of the power-splitting Simulink model. Note that to the left of section 7 in the above figure, the model is the same as that described in sections 1 and 2 in Annex A1 and A2.

B.2. Sections 6 & 7

Section 6 is exactly the same as described in figure 29 of Annex A6.

Section 7 is exactly the same as section 3 of annex A3, with the exception that the light green shaft at the right of the section does not terminate in a viscous damper (as it does in Annex A3, figure 25), but continues to section 8, described below.

B.3. Section 8

This section illustrates the major differences between the two Simulink models of Tordenskiold described in this report. On the left of Figure 33 below, the PTO shaft enters a planetary gear, which divides the mechanical power into two shafts of different gearing; the upper shaft is geared higher and turns a low-inertia, high-speed flywheel, whilst the lower shaft drives a high-inertia, low-speed shaft, and the generator (represented here by a viscous damper). The Two shafts are joined by a friction clutch, that is actuated by a control mechanism (described in the following section 9), driven by a hydraulic cylinder. In addition, a second friction clutch (lower right, green) serves to brake the generator shaft when necessary, allowing it to maintain a pre-set angular velocity whilst forcing additional incoming power to the high-speed shaft.

Note that the arrangement of these shafts and clutches is for illustrative purposes only. In practice, the shafts could be along the same axis (one rotating inside the other), as could the clutches.

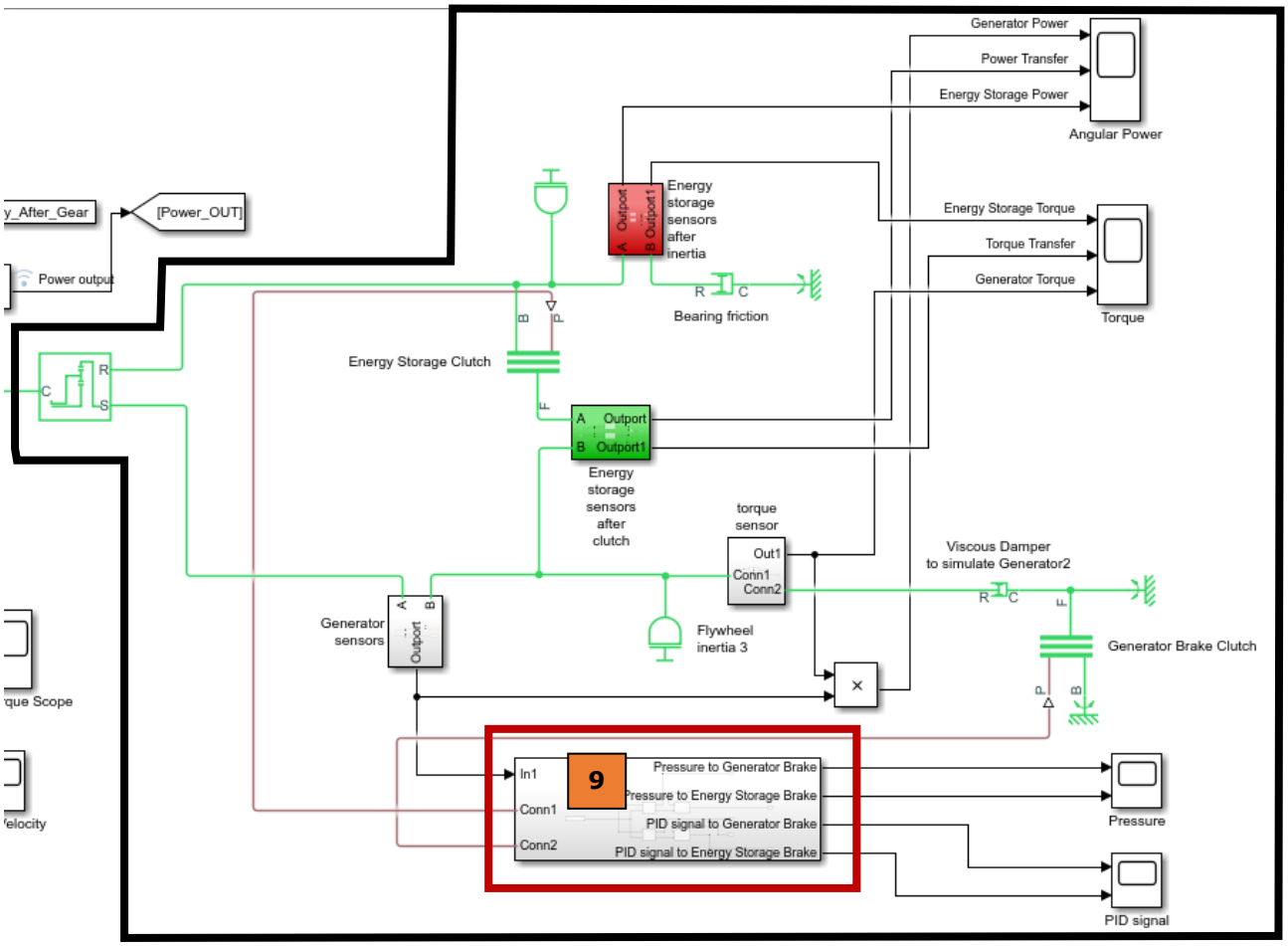

Figure 33. Section 8 of the power-splitting Simulink model. This features the two shafts attached to the ring and sun elements of the planetary gears, each with a flywheel, and one with the generator. The shafts are joined by an actively controlled friction clutch.

B.4. Section 9

This section has been masked (hidden) in the previous figures, but is expanded below. It comprises the logic system that controls the pressure in the hydraulic cylinders that drive both friction clutches. It is designed in such a way so that the clutches work in tandem, with only one applying a braking force at any time.

In the lower left is the desired speed (in RPM) which is compared against the measured signal (upper left, with a conversion from rad/s to RPM). The signal is then passed through a PID controller (section 10, described below) and a hydraulic actuator (section 11, described below) for each of the two friction clutches.

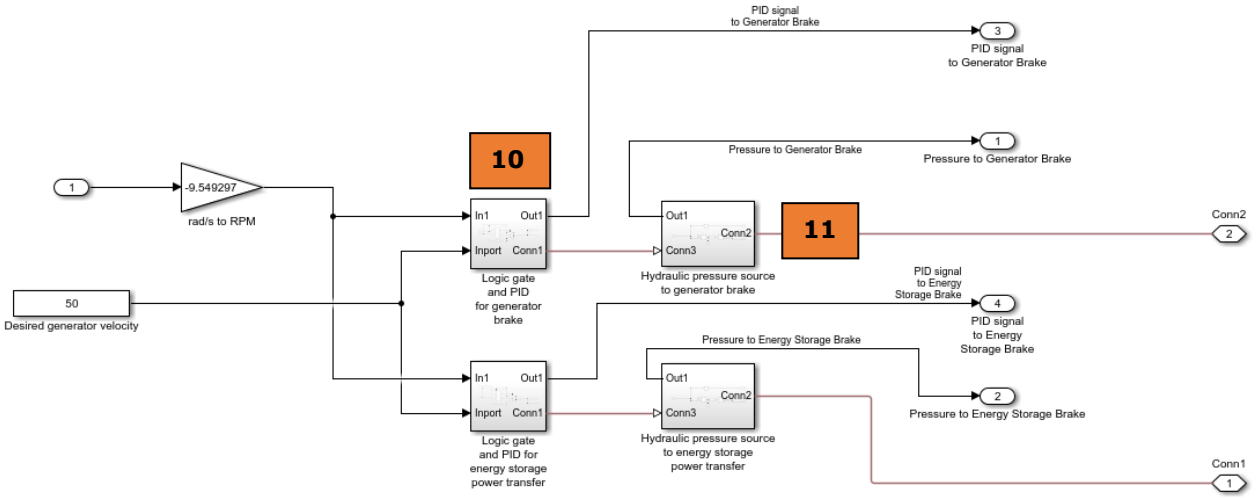

Figure 34. Layout of section 9, the masked control logic to activate the two clutches in order to maintain the generator shaft rotational velocity at the desired level.

B.5. Section 10

This section is a logic gate and PID (Proportional, Integral, Derivative) control system that compares the desired generator speed (input 2) to the actual generator speed (input 1), calculates the difference, and uses a PID controller to calculate the appropriate signal response send to the friction clutch hydraulic actuator (section 11). The signal is boosted by a constant value, passed through a signal delay (to prevent signal loops) and finally converted to a physical signal, which is passed to section 11 (labelled 'Conn 1', upper right).

Note that the output signal 1 (lower right) is passed to a scope in order to visualise the output signal and serves no other purpose.

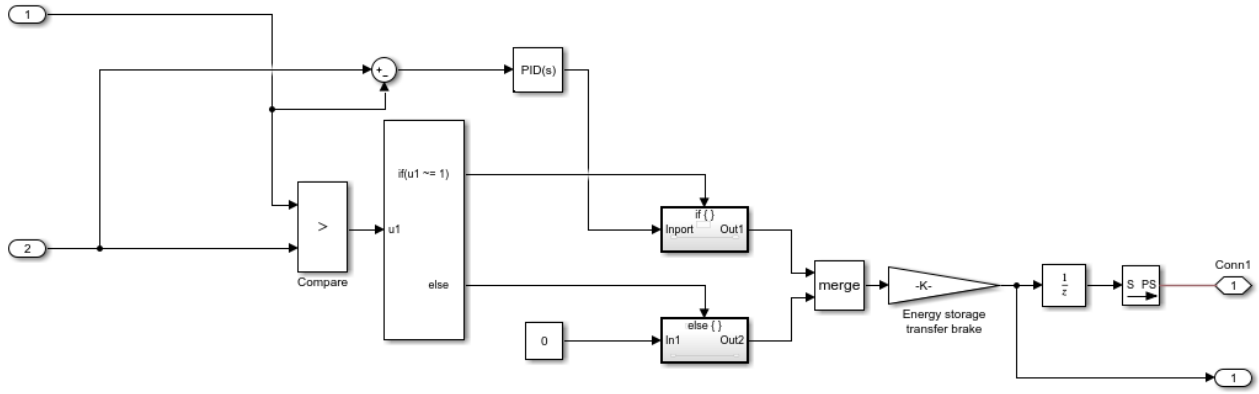

Figure 35. Layout of section 10, the masked PID control system that calculates the appropriate physical signal to relay to the friction clutch hydraulic system.

B.6. Section 11

This section represents an ideal hydraulic pressure source and sensor. The pressure source is ideal in the sense that it is capable of providing any pressure required to fulfil the demands of the simulation, and the sensor is ideal in that it does not affect the pressure.

In the lower right of the figure below is the input signal calculated by in section 10, which commands the pressure source to provide the corresponding hydraulic pressure to the friction clutch, connected to the physical output port labelled ‘Conn2’ (lower left). Also connected is a ‘PS-S’ block (‘physical signal to signal’) which is output from port 1 (upper right) to a scope for visualisation of the pressure signal.

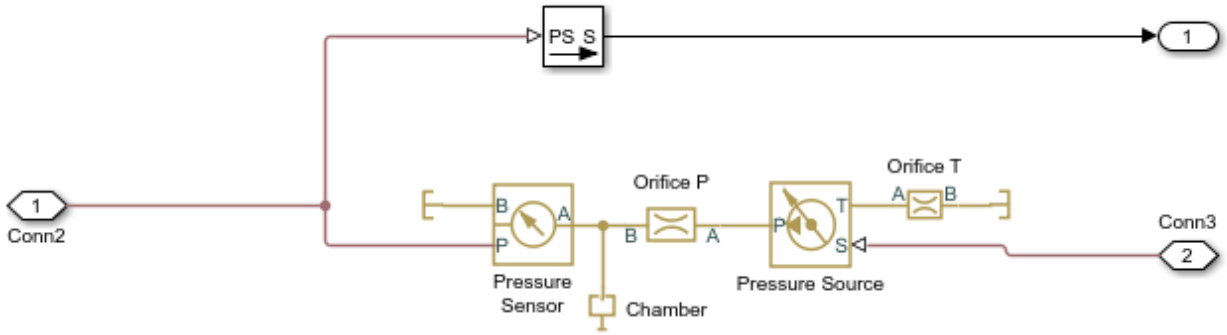

Figure 36. Layout of section 11, the masked hydraulic system that simulates the hydraulic pressure required to drive the friction clutch pistons.